國　立　交　通　大　學

電子工程學系 電子研究所碩士班

碩　士　論　文

以 ZrO_2 和聚合物做為 ISFET/REFET 之感測材料應用於讀出電路設計之特性與考量研究

The study of characteristics and considerations of ZrO_2 and polymer as ISFETs and REFETs sensing materials for the application of the readout circuits design

研 究 生：詹 仲 逸

指導教授：張 國 明 博士

中華民國九十八年八月

以 ZrO_2 和聚合物做為 ISFET/REFET 之感測材料應用於讀出電路設計之特性與考量研究

The study of characteristics and considerations of ZrO_2 and polymer as ISFETs and REFETs sensing materials for the application of the readout circuits design

研 究 生：詹仲逸　　Student：Chung-Yi Chan

指導教授：張國明 博士　　Advisor：Dr. Kow-Ming Chang

國 立 交 通 大 學

電子工程學系 電子研究所碩士班

碩 士 論 文

A Thesis

Submitted to Department of Electronics Engineering & Institute of Electronics

College of Electrical Engineering and Computer Engineering

National Chiao Tung University

In Partial Fulfillment of the Requirements

For the Degree of

Master

In

Electronics Engineering

August 2009

Hsinchu, Taiwan

中華民國九十八年八月

以 ZrO_2 和聚合物做為 ISFET/REFET 之感測材料應用於讀出電路設計之特性與考量研究

學生:詹仲逸　　指導教授:張國明 博士

國立交通大學

電子工程學系 電子研究所碩士班

摘　要

讀出電路的發展是為了微小化離子感測場效電晶體(Ion-sensitive Field Effect Transistor)的體積。讀出電路除了能夠微小化之外，它也擁有積體化和精確的輸出訊號的優點。為了能夠達簡便設計出電路的目的。我們必須對讀出電路中的高靈敏性的 ISFET 和低靈敏性的參考電晶體(REFET)這兩個基本元件有更多的了解。

在本篇論文中，我們先研究以二氧化鋯作為閘極的 ISFET。我們相當在意 ISFET 中兩樣重要的參數：靈敏度以及漂移。p 型的 ISFET 具有 57.08mV/pH 的靈敏度而 n 型的 ISFET 也具有 58.73mV/pH 的靈敏度。這種高的 ISFET 靈敏度能夠在量測中為我們帶來更高的判別度。除此之外，我們也對 ISFET 另一項重要參數：漂移有興趣。漂移指的是 ISFET 中臨限電壓的改變。當 ISFET 浸泡在化學溶液時，漂移就變成了一種必然發生的物理現象。在本篇論文中，我們提出一個可行的方法用來降低漂移量帶來的影響。藉著使用我們所提出的方式，最後確實成功的增加了訊號雜訊比例。

在研究的第二個部分，我們找到了一種合適的 REFET 材料。我們選擇了一種

Nafion 和 polyimide 比例為一比一的混合物，此種物質的靈敏度為 8.12 mV/pH 而飄移速率為 9.74 mV/hr。這種選定的材料在電導率上面的表現也和 ZrO_2 作為閘極之 ISFET 極為相似。上面提到的 REFET 特性：低的靈敏度、可接受的漂移速率、和 ZrO_2 作為閘極之 ISFET 匹配的電導率，都為我們在降低差動型 ISFET/REFET 讀出電路上的設計複雜度上帶來便捷的影響性。

The study of characteristics and considerations of ZrO_2 and polymer as ISFETs and REFETs sensing materials for the application of the readout circuits design

Student: Chung-Yi Chan Advisor: Dr. Kow-Ming Chang

Department of Electronics Engineering & Institute of Electronics

National Chiao Tung University

ABSTRACT

Readout circuit was developed to miniaturize the volume of ISFET (Ion-sensitive Field Effect Transistor). Besides the miniaturization, it also has advantages such as integration and the accurate output signal. To achieve the goal of design simplicity, we must know more about the basic devices including a high sensitive structure (ISFET) and a low sensitive structure (REFET).

In this thesis, we first investigated the ZrO_2 gate ISFET. We are interested in sensitivity and drift which are two important parameters for ISFET. The sensitivities are 57.08mV/pH for the p-type ISFET and 58.73mV/pH for the n-type ISFET respectively. The high sensitivity for the ISFET can bring the high resolution while measuring. Furthermore, we also interested in drift the other significant parameter of ISFET. Drift is the change of the threshold voltage of an ISFET. It is an unavoidable physical phenomenon while an ISFET immersed in the chemical solutions. To reduce the influence of drift, we introduce a feasible method in this thesis. We can successfully increase the signal-to-noise ratio with the use of the proposed method.

In the second part of this study, we found the suitable REFET material. We select the mixture of Nafion and polyimide with the 1/1 ratio of Nafion comparing to polyimide. The sensitivity and drift rate of this chosen material are 8.12 mV/pH and 9.74 mV/hr respectively. The transconductance of this material is also similar to the ZrO_2 gate ISFET. It is convenient for us to reduce the complexity of differential ISFET/REFET readout circuit because of the above properties of REFET.

誌　　謝

能夠在兩年內完成這篇論文，最要感謝的是張國明老師的幫助；無論是學術上的指導或日常生活上待人接物的道理，讓我在這兩年內除了專業知識之外也得到其他更多寶貴的東西。老師豁達的個性和對學生的提攜，為我帶來豐富的兩年碩士經驗，這兩年來真的是相當感謝老師對我的照顧。

此外要感謝的是王水進老師、鄧一中老師以及賴瓊惠老師，你們在口試中對本篇論文內容提出的建議及看法，除了讓本篇論文架構更為嚴謹之外，也提供了另一種思考問題的方式。

其次我要感謝張知天學長在實驗過程中給予的建議及鼓勵，使我對於實驗的內容更為了解，平常的交談中也傳授了許多的經驗談，令我受益匪淺。還要感謝鍾文駿學長對我的照顧，讓我適度的排解壓力和正確的調整自己的心態，以最好的狀態迎接這兩年來的種種挑戰。另外還要感謝庭嘉學長、秉燏、卓慶、汶錦及其他實驗室學長和同學，有了你們的協助，才讓我能夠順利的進行實驗，完成這一篇碩士論文。

最後要感謝我的父親詹勳乾先生，以及余庭英女士，在我的求學生涯中，你們開放的態度，讓我能夠自由自在的學習；遇到挫折失敗時，也都適時給予關心與幫助。感謝你們無怨無悔的付出，讓我能夠順利完成學業，取得碩士學位。

誌于　2009.08

詹仲逸

Contents

Abstract (in Chinese) ---------- i

Abstract (in English) ---------- iii

Acknowledgement ---------- v

Contents ---------- vi

Figure Captions ---------- viii

Table Captions ---------- xii

Chapter 1 Introduction

1.1 The reason to use ion-sensing-field-effect-transistor (ISFET) 1

1.2 Two kinds of electrodes---------- 2

1.2.1 The glass electrode---------- 2

1.2.2 The solid-state reference electrode---------- 3

1.3 The applications of ISFET : The readout circuit---------- 4

1.4 Motivation of this work and thesis---------- 5

1.5 References---------- 6

Chapter 2 Theory Description

2.1 The basic concepts and applications of pH---------- 8

2.2 Operating theory of ISFET---------- 8

2.2.1 The evolution from MOSFET to ISFET---------- 9

2.2.2 The surface between silicon dioxide and electrolyte---------- 10

2.2.3 The derivation of pH sensitivity of ISFET---------- 12

2.3 The drift phenomenon of ISFET---------- -------- 15

2.3.1 Dispersive transport to the hydration mechanism---------- 16

2.3.2 Expression for drift---------- 16

2.4 References---------- 19

Chapter 3 Experiment and Measurement

3.1 Introduction---------- 22

3.2 The fabrication process flow of ISFET and REFET---------- 22

3.3 The illustration of the core parts---------- 24

3.4 Measurement system---------- 25

3.3.1 Preparation before measurement---------- 25

3.4.2 The measurement of pH sensitivity---------- 26
3.4.3 The measurement of drift---------- 26
3.4 References---------- 27
Chapter 4 Results and Discussions
4.1 Introduction---------- 28
4.2 The p-type and n-type ISFET---------- 28
4.3 The results in the REFET structure---------- 30
4.4 Conclusions---------- 32
4.5 References---------- 32
Chapter 5 Future Work---------- 34

Figure Captions

Fig. 1-1 ISFET cross-section structure

Fig. 1-2 Important platform of Bio-sensors

Fig. 1-3 The electrode structures

Fig. 1-4 Conventional glass electrode

Fig. 1-5 Differential ISFET/REFET measuring system

Fig. 1-6 Direct (a) and indirect (b) feedback circuit

Fig. 1-7 Sketch of readout circuit with global feedback

Fig. 1-8 Sketch of an operational amplifier

Fig. 2-1 Structure of MOSFET and ISFET

Fig. 2-2 Site-binding model

Fig. 2-3 The interface between silicon dioxide and electrolyte

Fig. 2-4 Potential profile and charge distribution at an oxide electrolyte solution interface

Fig. 2-5 Schemat Gouy-Chapman-Stern model

Fig. 2-6 Series combination of the (a) initial (b) hydrated insulator capacitance

Fig. 3-1 Fabrication process flow

Fig 3-2 Chemical formula and sketch for Nafion

Fig. 3.3 Measurement set-up

Fig. 3-4 Detection principle of pH

Fig. 3-5 Detection principle of drift

Fig. 4-1 Id-Vg curve of ZrO_2 for p-type ISFET before drift

Fig. 4-2 Id-Vg curve of ZrO_2 for n-type ISFET before drift

Fig. 4-3 Time to drift in pH 3 buffer solution of p-type ISFEET for 400 minutes

Fig. 4-4 Time to drift in pH 5 buffer solution of p-type ISFEET for 400 minutes

Fig. 4-5 Time to drift in pH 7 buffer solution of p-type ISFEET for 400 minutes

Fig. 4-6 Time to drift in pH 9 buffer solution of p-type ISFEET for 400 minutes

Fig. 4-7 Time to drift in pH 11 buffer solution of p-type ISFEET for 400 minutes

Fig. 4-8 Time to drift in pH 3 buffer solution of n-type ISFEET for 400 minutes

Fig. 4-9 Time to drift in pH 5 buffer solution of n-type ISFEET for 400 minutes

Fig. 4-10 Time to drift in pH 7 buffer solution of n-type ISFEET for 400 minutes

Fig. 4-11 Time to drift in pH 9 buffer solution of n-type ISFEET for 400 minutes

Fig. 4-12 Time to drift in pH 11 buffer solution of n-type ISFEET for 400 minutes

Fig. 4-13 Time to drift rate of p-type ISFET in various buffer solution

Fig. 4-14 Time to drift rate of n-type ISFET in various buffer solution

Fig. 4-15 Comparison of drift amount between p-type and n-type ISFET in various buffer solutions

Fig. 4-16 Comparison of drift rate between p-type and n-type ISFET in various buffer solutions

Fig. 4-17 Selectivity of the HMDS/ZrO_2 structure

Fig. 4-18 Comparison of gm between ZrO_2 and the HMDS/ZrO_2 structure

Fig. 4-19 Comparison of gm between ZrO_2 and the test structures

Fig. 4-20 Selectivity of the PR/HMDS/ZrO_2 structure

Fig. 4-21 Time to drift in pH 7 buffer solution of the PR/HMDS/ZrO_2 structure for 400 minutes

Fig. 4-22 Sensitivity of the mixture (Nafion1:polyimide1)/HMDS/ZrO_2 structure

Fig. 4-23 Time to drift in pH 7 buffer solution of the mixture (Nafion1:polyimide1)/HMDS/ZrO_2 structure for 400 minutes

Fig. 4-24 Sensitivity of the mixture (Nafion1:polyimide3)/HMDS/ZrO_2 structure

Fig. 4-25 Time to drift in pH 7 buffer solution of the mixture (Nafion1:polyimide3)/HMDS/ZrO_2 structure for 400 minutes

Fig. 4-26 Sensitivity of the polyimide/HMDS/ZrO_2 structure

Fig. 4-27 Time to drift in pH 7 buffer solution of the polyimide/HMDS/ZrO_2 structure for 400 minutes

Fig. 4-28 Comparison of gm between ZrO_2 and the test structures

Table Captions

Table 1-1 Sensitivities and test range for different sensing membranes

Table 3-1 Specifications of wafers

Table 3-2 Parameters of sensing layers deposition with sputter

Table 3-3 The test structures of REFET, NF=Nafion, and PI=polyimide

Table 4-1 Sensitivity at the optimum operation current

Table 4-2 Comparison between original and modified S/N ratio

Table 4-3 Parameters of the test structures; NF=Nafion, PI=polyimide

Table 4-4 Parameters of the test structures; NF=Nafion, PI=polyimide

Chapter 1

Introduction

1.1 The reason to use ion-sensing-field-effect-transistor (ISFET)

Ion-sensing-field-effect-transistor (ISFET) was developed by P. Bergveld in the 1970s [1]. The important concept of the ISFET (shown in Fig. 1-1) was evolved from the metal-oxide-field-effect-transistor (MOSFET). We can use different sensing films to replace the gate electrode structure of MOSFET. From the electrochemical reaction between the sensing layer and the liquid electrolyte, the pH value can be detected. The parameter, pH value, plays an important role in many fields such as agricultural, chemistry, food chemistry, pharmaceutical industry and human health [2]. For example, the body fluid of living organisms usually has specific pH range. If the pH of the human blood changes by a little as 0.03pH units or less the functioning of the body will be greatly impaired [3].

In the early periods, an unstable reference voltage existed for the solution of measure, so the researchers added a stable reference electrode in succession to waiting for the solution of measure in the later researches. Furthermore, the choice of sensing layer is also an emphasis on the researches in the ISFET field because the SiO_2 is not an ideal film. To find a high sensitive and an obvious selective sensing layer is our objective. So the properties of (Table 1-1) ZrO_2 [4], Si_3N_4 [5], Al_2O_3 [6], Ta_2O_5 [7] and SnO_2 [8] sensing layer are investigated in the latter researches. With the studies to the sensing layers, we find some of them can detect specific ions such as K, Na, Ca ions. The ability to recognize the different ions is called as “Selectivity”. Because of the characteristic, ISFET can be used as a biosensor (shown in Fig. 1-2). Besides the

above discussions, it also owns some features. For instance, it can achieve the goal of the small size, strong robustness and rapid response. It is also compatible with the CMOS standard process nowadays. So it can have the lower cost.

1.2 Two kinds of electrodes

The instability is a serious drawback to ISFET. It would detect the incorrect pH value because of the non-ideal issue. From the researches of ISFET, it can utilize the electrodes to stabilize the electric potential in the liquid electrolyte. The most useful electrodes are glass electrode and solid-state electrode shown as Fig. 1-3.

1.2.1 The glass electrode

The first glass electrode is invented by Cremer in 1906. Thereafter, the published researchers focus on the improvement in its application. The major element of the glass electrode is a bulk of glass membrane providing the pass channels for hydrogen ions. Inside the glass membrane is a fixed concentration of HCl or a buffered chloride solution contact with an internal Ag/AgCl reference electrode. We can see the diagram in Fig. 1-4.

The immersion in the chemical buffer solution of the glass electrode can produce the way to transfer ions in the surface of the glass bulk. The transfer reaction for hydrogen ions is the result to the hydration of the surface of the glass membrane. It can not only build up hydrogen ions layer but also stabilize the electric potential [9]. For the reason of the stable voltage, the various components such as Na_2O-CaO-SiO_2, Li_2O-BaO-SiO_2, Li_2O-Cs_2O-La_2O_3-SiO_2, are doped to the glass material [10]. For example, the alkali oxide (ex. $Li_XSi_YO_Z$; alkali silicon dioxide compound) will break

the stable Si-O bond and lead to the change between Li^+ and H^+:

$$SiO^- Li^+ (glass_membrane) + H^+ (solution)$$

$$\rightarrow SiO - H + (hydrated_layer) + Li^+ (solution)$$

Li^+ produce charges and these charges consequently build up the surface potential. From the Nernst equation, we can know that activity of hydrogen ions is related with the surface potential and can easily calculate the potential difference between the outside and inside glasses. The Nernst equation is listed as the following equation.

$$E = Eo + \frac{RT}{nF} \ln \alpha_{H^+}$$

where E = electrode potential, E_0 = standard potential of the electrode, R = gas constant ($8.31441 JK^{-1}mol^{-1}$), T = temperature (in Kelvin), n = valance (n=1 for hydrogen ions), F = Faraday constant and α_{H^+} = activity of hydrogen ions.

According to the equation, providing that at one side of the interface the activity of the ion of interest is kept constant, the electrode potential is a direct logarithmic function of the ion activity on the other side [10]. And then we can easily define a stable potential suggesting that no interference reaction will occur. The most attractive advantage is established. Because of the advanced IC fabrication techniques, the ISFET-based pH sensor has a big potential for widely application and becomes a new choice for pH detection.

1.2.2 The solid-state reference electrode

As the extensive applications of ISFET, the inconvenience of its large size is also discussed. So we can use the solid-state reference electrode to replace the past glass electrode. The solid-state reference electrode is composed of noble metal such as Ag, Pt, et al. The noble materials are often steady and difficult to react in the aqueous

solutions. But it is unable to produce the same ion-exchange reactions like glass electrode. There is no stable electric potential in the solid-state reference electrode because of the unstable ion-absorbing reaction causing in the metal surface. Some methods are published to solve this problem [11] (Shown in Fig. 1-5). The specific manner is utilizing two ISFET, one of them is high sensitivity and the other one with low sensitivity is called as REFET (Reference Field Effect Transistor). REFET is identical with ISFET except that REFET does not react on the ion concentration to be measured, i.e. REFET is insensitive to the test ion concentration [11]. Even in the identical conditions, ISFET and REFET produce two different voltages. This circuit topology and the use of differential operation amplifier can eliminate the common influences created from the solid-state reference electrodes of ISFET and REFET.

The origin of the instability may be the redox reaction or other reactions at noble metal reference electrode and the liquid interface, i.e. the liquid/solid interface. So elimination or reduction of the unstable measured voltage is the focus of investigating the solid-state reference electrode.

1.3 The applications of ISFET: The readout circuit

We could miniaturize the size of ISFET by introducing solid-state electrode. ISFET with solid-state is able to detect the existence and concentration of different ions by itself, but there is an issue of the degree of the accuracy in this case. Generally, a slight degree of the measurement deviation can be adopted. But in some situations of the strict requisitions, such as a health examination or a quarantine of the agricultural products, the measurement accuracy is indispensably necessary. There are two important essentials in the biomedical sensors including the accurate output signal and the stable biasing current and voltage. So the specific circuits are

continuously investigated [11]. Furthermore, the functions of the novel readout circuits are getting more and more as the development of fabrication and the circuit topologies. Nowadays, we can achieve a lot of goals including the low power consumption, reduction the amount of drift and the linearity of the output signal, in only single readout circuit. We can see these circuit sketches in Fig. 1-6 [12] and Fig. 1-7 [13].

Today, we want to produce a wonderful pH sensor with small size and the ability of continuous monitoring. Therefore, the investigations on the part of the readout circuit are getting more and more significant. Low power consumption, the accuracy of measurement results, elimination of influences in the surrounding, the small layout area of the readout circuit, and simplification of design are all our targets. To achieve and combine these benefits in single readout circuit is an important fundamental for the glorious pH sensors.

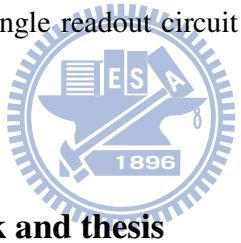

1.4 Motivation of this work and thesis

Readout circuit could miniaturize the pH-ISFET measurement and provide the accurate output signal. As mentioned before, the unstable issue of the measurement still exists until now. There are many methods to solve the problem. At first, we try to improve the performances of the ISFET. But the result is unapparent. So the researchers focus on the readout circuits. According to Ref. [14], it is an achievable method to reduce the instability obviously. Besides the stability, we can obtain the other advantages at the same time in the present days.

In the readout circuits, we can see the various parts of ISFET-REFET pair, ISFET-MOSFET pair or the arbitrary combinations with the three different devices, no matter the functions of the circuit are identical or different. Besides the pairs,

operation amplifiers are usually used. A normal operation amplifier is shown as Fig. 1-8 [14].

The study is interested in the characteristics of the fundamentals in the readout circuits including ZrO_2 gate ISFETs and polymer based REFETs. From the measured data, we are able to improve the original circuit with the introduction of some specific compensation circuits. We could also use the property of the two devices, the circuit topology, and the feedback concept to stabilize the output voltage and to obtain the better performances from the novel readout circuits in the future.

In chapter 2, the basic theories and non-ideal phenomenon of ISFET are introduced. And the detail process flow of this experiment will be listed in chapter 3. In chapter 4, we will have some discussions about our experimental results and in chapter 5, the future work of this experiment is presented.

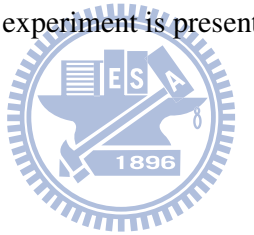

1.5 References

[1] P. Bergvled,"Development of an ion-sensitive solid-state device for neurophysiological measurement", *IEEE Trans. On Bio-Med. Eng.* (1970) 70-71

[2] H. Kaden, H. Jahn, M. Berthold, "Study of the glass/polypyrrole interface in an all-solid-state pH sensors", *Solid State Ionics*, vol. 169, pp. 129-133, 2004.

[3] Y. Q. Miao, J. R. Chen and K. M. Fang, "New technology for the detection of pH", *J. Biochem. Biophys. Methods*, vol. 63, pp. 1-9, 2005.

[4] K. M. Chang, K. Y. Chao, T. W. Chou, and C. T. Chang, "Characteristics of Zirconium Oxide Gate Ion-sensitive Field-Effect Transistors", *Japanese Journal of Applied Physics* Vol. 46 No. 7A pp. 4334-4338 2007.

[5] H. K. Liao, J. C. Chou, W. Y. Chung, T. P., and S. K. Hsiung, "Study on the interface trap density of the Si_3N_4/SiO_2 gate ISFET", *Proceeding of the Third East*

Asian Conference on chemical Sensor, Seoul, South Korea, pp. 394-400, Nov 1997.

[6] S. Jamasb, S. D. Collins, R. L. Smith, "A Physically-based Model for Drift in Al_2O_3-gate pH ISFETs " in *International Conference on Solid-State Sensors and Actuators* Chicago, June, 1997.

[7] P. Gimmel, B. Gompf, D. Schmeiosser, H. D. Weimhofer, W. Gopel, and M. Klein, "Ta_2O_5 gate of pH sensitive device comparative spectroscopic and electrical studies", *Sensors and Actuators B* vol. 17 pp. 195-202, 1989.

[8] Y. Q. Miao, J. R. Chen and K. M. Fang, "New technology for the detection of pH", *J. Biochem. Biophys. Methods*, vol. 63, pp. 1-9, 2005.

[9] 董勝敏, 王承遇, 潘玉昆, "pH 玻璃電極的現狀與發展", *GLASS & ENAMEL*, vol. 32, No. 2, pp. 54-57, Feb. 2004.

[10] P. Bergveld, "ISFET, Theory and Practice", in *IEEE Sensor Conference,* Toronto, Oct. 2003.

[11] P. Bergveld, "Thirty years of ISFETOLOGY What happened in the past 30 years and what happen in the next 30 years", *Sensors and Actuators B*, vol. 88, pp. 1-20, 2003.

[12] U. Dinnar, Claudio G. Jackobson, "CMOS Readout Circuit for Biomedical ISFET-Based Microsystems", *The 16th Europaen Conference on Solid-State Transducers*, Prague, Czech Republic, Sepetember 15-18, 2002.

[13] B. Premanode, N. Silawan, W. P. Chanc, and C. Toumazoua, "A composite ISFET readout circuit employing current feedback", *Sensors and Actuators B*, vol. 127, pp. 486-490, 2007.

[14] Yang Zhen, Yan Yong-hong, and Qi Liang-jie, "A Integrated pH-ISFET Sensor With CMOS Technology", *Semiconductor Technology*, vol. 29, No. 12, pp. 56-59, Dec. 2004.

Chapter 2

Theory Description

2.1 The basic concepts and applications of pH

The two letters, “pH”, is an abbreviation of the potential of Hydrogen. About 100 years ago, 1909, the concept of pH was published by Danish chemist S. P. L. Sørensen [1]. pH is an important parameter for determining the acidity or alkalinity of different unknown chemical solutions. Solutions are considered acidic with a pH less than seven, while those with pH greater than 7 are considered alkaline. pH 7, the standard between the acid and alkaline solutions, is defined as neutral because of the equality of the concentration of H_3O^+ and the concentration of OH^- at 25℃ in the pure water at the specific pH value [2]. pH also plays an important role in several kinds of domains such as agricultural, chemistry, food chemistry, pharmaceutic industry and human health [3].

We can use the following formula to find out the pH value we needed. The formula used to calculate pH value is defined as:

$$pH = -\log_{10} \alpha[H^+] \tag{2-1}$$

where α is the activity coefficient and $[H^+]$ is the molar concentration of solvated protons in units of moles per liter (moles/L). From equation (2-1), we can know that pH value related to the amount of available hydrogen ions not the concentration of hydrogen ions.

2.2 Operating theory of ISFET

Ion-selective field effect transistors (ISFETs) were first published by P. Bergveld in the 1970s. Besides the structure of the gate, the other parts of ISFETT are similar to MOSFET (Metal Oxide Semiconductor Field Effect Transistor). The gate electrode of ISFET is substituted for a reference electrode and immersed in an undefined solution contacted with the gate sensing layer. The first purple of using a reference electrode is that a capacitor (with the gate oxide as the dielectric material) needs two parallel plates for connecting. The two parallel are respectively the silicon substrate and the electrolyte [4]. The second reason of the existence of the reference electrode is stable while ion transferring. Without the reference electrode, the electrolyte potential is getting more unstable and easily disarranged by the disturbances from the surrounding. We can know the main function of ISFET is measuring the concentration of various kinds of ions in different chemical liquid solutions from the above-mentioned reasons. A schematic structure of MOSFET and ISFET are shown in Fig. 2-1.

2.2.1 The evolution from MOSFET to ISFET

The concept of ISFET comes from MOSFET. So the fundamental framework, geometric structure, and the theories of operating, are almost similar. We usually bias ISFET in the linear region. So we can get the expression of ISFET from the same biasing condition of MOSFET. For both MOSFET and ISFET, the drain current in the triode region is:

$$I_D = \mu C_{OX} \frac{W}{L}\left\{(V_{GS} - V_t) - \frac{1}{2}V_{DS}\right\}V_{DS} \qquad (2\text{-}2)$$

where C_{ox} is the oxide surface capacitor in the unit of F/Cm^2, and μ is the mobility of the majority carriers in the channel region. W and L are the denotations of the width and length of the channel respectively. An useful parameter, β, defined as

$\beta = \mu C_{ox} \frac{W}{L}$, plays an important role in the field of designing electrical circuits. From the advanced process steps and ideal circuit design, we can make the threshold voltage V_t and the drain-source voltage V_{DS} almost const. Thus the drain current I_D is direct proportion to the V_{GS} in MOSFET.

The V_t term in equation (2-2) can be calculated as shown in equation (2-3).

$$V_t = \frac{\phi_M - \phi_{Si}}{q} - \frac{Q_{OX} + Q_{SS} + Q_B}{C_{OX}} + 2\varphi_F \qquad (2\text{-}3)$$

where ϕ_M is the work-function of the metal gate, ϕ_{Si} is the work-function of silicon, Q_{ox} is the accumulated charge in the oxide, Q_{ss} is the surface charge density between oxide and silicon surface, Q_B is the depletion charge in the silicon and φ_f is Fermi-potential [5].

In the case of ISFET, the metal gate is taken off [2]. The expression of threshold voltage is needed to modify. The interface between the solution and the gate oxide and the interface between solution and the reference is considered [6]. It is shown as below:

$$V_t = E_{ref} + \chi^{sol} - \Psi_0 - \frac{\Phi_{Si}}{q} - \frac{Q_{OX} + Q_{SS} + Q_B}{C_{OX}} + 2\varphi_F \qquad (2\text{-}4)$$

The term is the reference electrode potential related to vacuum level E_{ref}, which includes ϕ_M, χ^{sol} is the surface dipole potential of the solution, which is a constant. All terms are constant except Ψ_0, it is the kernel of ISFET sensitivity to the electrolyte pH value which is controlling the dissociation of the oxide surface. The way to gain a pH sensitive ISFET is to concentrate on the surface between oxide and solution. The detailed investigations in the oxide-electrolyte interface are able to help us to find out the best oxide instead of a priori silicon dioxide as used for MOSFETs [6].

2.2.2 The surface between silicon dioxide and electrolyte

There is a chemical reaction in the part of oxide-electrolyte interface [4][6][7]. The sketches of the reaction are illustrated as Fig. 2-2, Fig. 2-3, and Fig. 2-4. We can explain the reason of the phenomenon as the SiO_2 sensing layer. The silicon hydroxyl groups contained in the surface of the oxide sensing layer can donate or accept a proton from the electrolyte. The chemical reaction will build up charges and develop the electrical potential in the region. The phenomenon can be explained with the site-binding model introduced from by Yate et al [8]. The statement can describe the interface with the combination and generation of protons from the silicon hydroxyl groups. The neutral sites may become negatively charged or positively charged surface groups respectively by donating or accepting protons. The surface reactions are:

$$SiOH \xleftrightarrow{K_a} SiO^- + H_S^+ \tag{2-5}$$

$$H_S^+ + SiOH \xleftrightarrow{K_b} SiOH_2^+ \tag{2-6}$$

where H_S^+ represents the protons in the at the surface of the oxide, K_a and K_b are the chemical equilibrium constants. Eq. (2-5) and Eq. (2-6) imply the surface chemical reaction dynamically equilibrated, too.

The proton concentration distribution is affected by the potential between the oxide sensing layer and the chemical solution, and according to the Boltzmann [9]. The Boltzmann equation is stated as the following equations:

$$a_{H_S^+} = a_{H_B^+} \exp\left(\frac{-q\psi_o}{kT}\right) \tag{2-7}$$

or in the from of pH

$$pH_S = pH_B + \frac{q\Psi_0}{2.3KT} \tag{2-8}$$

where $a_{H_S^+}$ and $a_{H_s^+}$ are the activity of H_S^+ at the oxide surface and the bulk of the solution respectively, k is the Boltzmann constant, T is the absolute temperature, ψ_o is the surface potential, pHs is the pH value at the oxide surface, pH_B is the pH value in the bulk of the solution, q is the element charge.

2.2.3 The derivation of pH sensitivity of ISFET

To derivate the pH value, we should know the surface density of the amount of the surface site N_S and the surface charge density σ_0 (C/m^2). They are shown as below equations.

$$N_S = v_{SiOH} + v_{SiO^-} + v_{SiOH_2^+} \tag{2-9}$$

$$\sigma_0 = (v_{SiOH_2^+} + v_{SiO^-}) = -qB \tag{2-10}$$

where v_{SiOH2+}, v_{SiO-} and B is the symbol of the number of positively charged, negatively charged, neutral groups in mole per unit area respectively [5]. From Ref. [2] [6], the detailed derivation of σ_0 can be found.

$$\sigma_o = qNs\left(\frac{a_{H_S^+}{}^2 - K_aK_b}{K_aK_b + K_ba_{H_S^+} + a_{H_S^+}{}^2}\right) \tag{2-11}$$

where K_a and K_b are dissociation constant. We can get the intrinsic buffer capacity β_{int} after taking the differential to σ_0 with the variable pH. β_{int} is also the function of the activity of surface H^+-ions.

$$\frac{\partial\sigma_o}{\partial pH_S} = -q\frac{\partial B}{\partial pH_S} = -q\beta_{\text{int}} \tag{2-12}$$

We can obtain β_{int} for combining equation (2-11) and (2-12).

$$\beta_{\text{int}} = N_S\frac{K_ba_{H_S^+}{}^2 + 4K_aK_ba_{H_S^+} + K_aK_b{}^2}{\left(K_aK_b + K_ba_{H_S^+} + a_{H_S^+}{}^2\right)^2}2.3a_{H_S^+} \tag{2-13}$$

In this case, it is capable of buffering small changes in surface pH (pH_S) only and is not in bulk pH (pH_b), so it is called intrinsic. And N_S, K_a and K_b are related to oxide. To hydrolyze the surface will create more surface sites which can make the intrinsic buffer capacity and the sensitivity more [6].

According to the charge neutrality, the surface charge σ_o is balanced by an equal but opposite charge, σ_{dl}, in electrolyte. The two opposite charges, σ_o and σ_{dl}, parallel to each other form the electrical double layer structure, and the integral electrical double-layer capacitance is named $C_{dl,i}$. The relation between them is

$$\sigma_{dl} = -\sigma_o = -C_{dl,i} \times \psi_o \tag{2-14}$$

where the potential of the suface to the bulk of solution is $\psi_o = \psi_s - \psi_B$ [6]. The figure of the Gouy-Chapman-Stern model is shown as Fig. 2-5. We can calculate the integral double-layer capacitance $C_{dl,i}$ with the Gouy-Chapman-Stern model [10]. The Gouy-Chapman-Stern model involves a diffuse layer of charge in the solution and starts at a distance of x_E from the surface. A series network of the Helmholtz-layer capacitance (the Stern capacitance) and a diffusion layer capacitance is composed of the double-layer capacitance. And the charge in the diffusion layer, σ_{dl}, is calculated as:

$$\sigma_{dl} = -\sqrt{8kT\varepsilon_r\varepsilon_0 n^0}\sinh\left(\frac{zq\phi_E}{2kT}\right) \tag{2-15}$$

where ϕ_E is the potential at x_E, n^0 is the total concentration of each ion in the bulk solution, z is the valence number of the ions., and the parameters ε_r, ε_0, k, q and T are their normal meanings.

According the Kirchhoff's Voltage Law, we know the voltage drop across the Stren capacitance equaled with the difference between the potential ψ_1 at Y_T and the surface potential ψ_0. Therefore the potential ψ_1 can be described by:

$$\psi_1 = \psi_0 - \frac{\sigma_0}{C_{Stren}} = \psi_0 - \frac{\sigma_0 x_E}{\varepsilon_r \varepsilon_0} \tag{2-16}$$

So we can express the integral double-layer capacitance with the variables ψ_0 and the electrolyte concentration from Eq. (2-13) and Eq. (2-14). The ability of the double layer to store charges, which is defined in response to a small charge in the potential $\partial\sigma_0 / \partial\psi_0$, is denoted as C_{dif}, and calculated:

$$\frac{\partial \sigma_0}{\partial \psi_0} = -\frac{\partial \sigma_{dl}}{\partial \psi_0} = C_{dif} \tag{2-17}$$

We can achieve the purpose of simplicity for taking the expression for the inverse C_{dif}. Eq. (2-18) clearly shows that this capacitance is composed of two components in series:

$$\frac{1}{C_{dif}} = \frac{\partial \psi_0}{\partial \sigma_0} = \frac{1}{C_{Stren}} + \frac{1}{\sqrt{\frac{2\varepsilon_r \varepsilon_0 z^2 q^2 n^0}{kT}} \cosh(\frac{zq\psi_1}{2kT})} \tag{2-18}$$

It shows that the effect of a small change in the surface *pH* (pH_s) on the change in the surface potential ψ_0 to combine Eq. (2-12) and Eq. (2-17):

$$\frac{\partial \psi_0}{\partial pH_S} = \frac{\partial \psi_0}{\partial \sigma_0} \cdot \frac{\partial \sigma_0}{\partial pH_S} = \frac{-q\beta_{\text{int}}}{C_{dif}} \tag{2-19}$$

Rearrange Eq. (2-19) gives the general expression for pH sensitivity of an ISFET of the electrostatic potential to changes in the bulk [2]:

$$\frac{\partial \psi_0}{\partial pH_B} = -2.3\frac{kT}{q} \cdot \alpha \tag{2-20}$$

where

$$\alpha = \frac{1}{\frac{2.3kTC_{diff}}{q^2 \beta_{\text{int}}} + 1} \tag{2-21}$$

The dimensionless sensitivity parameter α, which varies between 0 and 1, is associated with the intrinsic buffer capacity β_{int} and the double-layer capacitance C_{dif}. The parameter α is almost equal unity when β_{int} is extreme large and C_{dif} approaches zero. The ISFET has a so-called Nernstian sensitivity of precisely -59.2mV/pH at 298K, which is also the maximum achievable sensitivity. The ordinary

SiO_2 film compatible with the standard CMOS fabrication process flow can not fit the requirements of a high value of β_{int}. In the condition, the pH sensitivity is only about 30mV/pH. So it is impossible to find the high sensitivity sensing films. These materials included high sensitivity have been investigated such as Si_3N_4 [11][12], Al_2O_3 [13][14], Ta_2O_5 [11][14], HfO_2 [14], and SnO_2 [15].

2.3 The drift phenomenon of ISFET

The phenomenon called as drift is a change of the threshold voltage of an ISFET. It is difficult to identify the cause of this phenomenon, which could be either a surface or a bulk effect, or both. The trap of hydrogen-bearing species can be considered as the surface effect, and the hydration of the insulator after immersed in pH solution can be categorized as the bulk effect. And the followings are the possible causes of drift [16].

(1) Injection of electrons from the electrolyte at strong anodic polarizations created negative space charge inside sensitive film.

(2) Some surface effects, such as the rehydration of a surface that is partially dehydrated and ion exchange involving OH^- ions.

(3) Variation of the surface state density (D_{it}) at the Si/SiO_2 interface which means the drift dependence of diffusion mechanism.

(4) Drift of sodium ion under the influence of the insulator field. Given an effective diffusion coefficient D_{eff} , it is clear that a bulk redistribution of sodium which has left a trap near the edge of the SiO_2.

2.3.1 Dispersive transport to the hydration mechanism

According to Ref. [16], we can know the two kinds of the drift mechanisms, the surface effect and the bulk effect to the various sensing layers. The concept of the trap of hydrogen-bearing species can be seen as the application of the site-binding model. In 1998, Jamasb proposed a physical model quantitatively to explain drift in terms of the bulk effect, hydration of the silicon nitride surface [17].

It is known that the drift phenomenon of an ISFET is modeled by implementing a hopping transport mechanism, known as dispersive transport [18] [19], to determine the rate of hydration of the sensing layer. We can see the dispersive transport in a broad class of disordered materials. Dispersive transport leads to a characteristic power-law time decay of diffusivity [20] which can be described as:

$$D(t) = D_{00}(\omega_0 t)^{\beta-1} \tag{2-22}$$

where D_{00} is a temperature-dependent diffusion coefficient which obeys an Arrhenius relationship, ω_0 is the hopping attempt frequency, and β is the dispersion parameter satisfying $0 < \beta < 1$. In turn, dispersive transport also leads to decay in density of sites/traps occupied by the species undergoing transport [20]. This decay is described by the stretched-exponential time dependence given by:

$$\Delta N_{S/T}(t) = \Delta N_{S/T}(0)\exp[(-t/\tau)] \tag{2-23}$$

where $\Delta N_{S/T}(t)$ is the area density (unit of cm^{-2}) of sites/traps occupied, τ is the time constant combined with structural relaxation, and β is the dispersion parameter.

2.3.2 Expression for drift

It is important to keep the biasing current constant while operating an ISFET. We

can achieve the purpose easily in the normal condition. But the sensing layer is getting hydrated all the time when the electrode is immersed in the aqueous electrolyte. The hydration makes the chemical composition of the sensing layer different from that of the bulk of the sensing material. Consequently, the dielectric constant is dissimilar to that of the un-hydrated layer. The equivalent insulator capacitance is also determined by the series combination of the surface hydration layer and the underlying sensing film, will exhibit a slow, temporal change. When the ISFET is biased in the region we need, the gate voltage will simultaneously exhibit a change to keep a constant drain current. The change of the gate voltage can be written as [21]:

$$\Delta V_G(t) = V_G(t) - V_G(0) \tag{2-24}$$

Since the voltage drop inside of the semiconductor is kept a constant, $\Delta V_G(t)$ becomes:

$$\Delta V_G(t) = [V_{FB}(t) - V_{FB}(0)] + [V_{ins}(t) - V_{ins}(0)] \tag{2-25}$$

where V_{FB} is the flat-band voltage and V_{ins} is the voltage drop across the insulator. V_{FB} and V_{ins} are given by the following expression:

$$V_{FB} = E_{ref} + \chi^{sol} - \Psi_0 - \frac{\Phi_{Si}}{q} - \frac{Q_{OX} + Q_{SS}}{C_{OX}} \tag{2-26}$$

$$V_{ins} = \frac{-(Q_B + Q_{inv})}{C_{OX}} \tag{2-27}$$

where the Q_{inv} is the inversion charge. If the pH, temperature, and the ionic strength of the solution are kept constants, E_{ref}, Φ_{Si}, Ψ_0, and χ^{sol} can be neglected, so the drift an be rewritten as:

$$\Delta V_G(t) = -(Q_{OX} + Q_{SS} + Q_B + Q_{inv})[\frac{1}{C_i(t)} - \frac{1}{C_I(0)}] \tag{2-28}$$

In our study, the gate oxide of the fabricated ISFET was consist of two layers, a lower layer of thermally-grown SiO_2 of thickness, t_L, and an upper layer of

sputter-grown ZrO_2 of thickness, t_U. $C_I(0)$ is the effective insulator capacitance given by the series combination of the thermally-grown SiO_2 capacitance, ε_L/t_L, and the sputter-grown ZrO_2 capacitance, ε_U/t_U. $C_i(t)$ is analogous to $C_I(0)$, but an additional hydrated of capacitance make C_i always smaller than C_I, ε_{HL}/t_{HL}, at the oxide-electrolyte interface must be considered, and the sputter-grown ZrO_2 capacitance is now given by $\varepsilon_U/[t_U - t_{HL}]$. The series combinations of the capacitance are illustrated in Fig. 2-6. Therefore, the drift is given by:

$$\Delta V_G = -(Q_{OX} + Q_{SS} + Q_B + Q_{inv})\left[\frac{\varepsilon_U - \varepsilon_{HL}}{\varepsilon_U \varepsilon_{HL}}\right] t_{HL}(t) \tag{2-29}$$

From this equation, we can know that the drift of gate voltage ΔV_G if the substrate type was different, it is depend on the Q_{inv} and Q_B. Other terms at Eq. (2-29) can be seen as constant value no matter what the substrate is. According to this assume, it is possible to eliminate the drift or hold the drift to be a constant at any other pH aqueous solution through the CMOS ISFET. By applying dispersive transport theory, an expression for $t_{HL}(t)$ is given by [22]

$$t_{HL}(t) = t_{HL}(\infty)\left\{-\exp\left[-(t/\tau)^{\beta}\right]\right\} \tag{2-30}$$

with

$$t_{HL}(\infty) = \frac{D_{00}\omega_0^{\beta-1}\Delta N_{S/T}(0)}{A_D \beta N_{hydr}} \tag{2-31}$$

where A_D is the cross-sectional area, and N_{hydr} is the average density of the hydrating species per unit volume of hydration layer. Hence, combination of eqns.2-24 to eqns.2-30 the gate voltage drift can be expressed by the following equation:

$$\Delta V_G(t) = -(Q_{OX} + Q_{SS} + Q_B + Q_{inv})\left[\frac{\varepsilon_U - \varepsilon_{HL}}{\varepsilon_U \varepsilon_{HL}}\right] t_{HL}(\infty)\left\{1-\exp\left[-(t/\tau)^{\beta}\right]\right\} \tag{2-32}$$

According to Eq. (2-32), we can know that if the immersing time of the gate oxide is long enough, the shift of gate voltage will approach almost a constant value which is greatly dependent on the hydration depth, $t_{HL}(\infty)$.

2.4 References

[1] Y. Q. Miao, J. R. Chen and K. M. Fang, "New technology for the detection of pH", *J. Biochem. Biophys. Methods*, vol. 63, pp. 1-9, 2005.

[2] P. Bergveld, "ISFET, Theory and Practice", in *IEEE Sensor Conference,* Toronto, Oct. 2003.

[3] H. Kaden, H. Jahn, M. Berthold, "Study of the glass/polypyrrole interface in an all-solid-state pH sensors", *Solid State Ionics*, vol. 169, pp. 129-133, 2004.

[4] P. Bergveld, "Thirty years of ISFETOLOGY What happened in the past 30 years and what happen in the next 30 years", *Sensors and Actuators B*, vol. 88, pp. 1-20, 2003.

[5] H.K. Liao, et al. "Study on pH_{pzc} and surface potential of tin oxide gate ISFET", *Materials Chemistry and Physic*s, vol. 59, pp. 6-11, 1999

[6] R.E.G. van Hal et al. , "A general model to describe the electrostatic potential at electrolyte oxide interface", *Advance in Colloid and Interface Science*, vol.69, pp. 31-62, 1996.

[7] Miao Yuqing , Guan Jianguo, Chen Jianrong, "Ion sensitive field transducer-based biosensors", *Biotechnology Advances*, vol. 21, pp. 527-534, 2003.

[8] D. E. Yates, S. Levine, and T. W. Healy, "Site-binding model of the electrical double layer at oxide/water interface", *J. chem. Soc. Faraday Trans. I*, vol. 70, pp. 1807-1818, 1974.

[9] W. M. Siu, R. S. C. Cobbold, "Basic Properties of the Electrolyte-SiO2-Si System:

Physical and Theoretical Aspects", *IEEE Transactions on Electron Device*, vol. ED-26, NO. 11, Nov., 1979

[10] 吳浩青, 李永舫, " 電化學動力學", 科技圖書公司, 2001 年 2 月

[11] Tadayuki Matsuo, Masayoshi Esashi, "Methods of ISFET Fabrication", *Sensors and Actuators*, vol. 1, pp. 77-96, 1981.

[12] Imants R. Lauks, Jay N. Zemel, "The Si3N4/Si Ion-Sensitive Semiconductor Electrode ", *IEEE Transactions on Electron Devices*, vol. ED-26, no.12, pp. 1959- 1964, Dec., 1979.

[13] J. C. Chou, C. Y. Weng, "Sensitivity and hysteresis effect in AL2O3 gate pH-ISFET", *Materials Chemistry and Physics*, vol. 71, pp. 120-124, 2001.

[14] P.D. van der Wal et al. ,"High-K Dielectrics for Use as ISFET Gate Oxide", in *Sensors, Proceedings of IEEE.2004*

[15] H. K. Liao et al., "Study of amorphous tin oxide thin films for ISFET applications", *Sensors and Actuators B*, vol.50, pp. 104-109, 1998.

[16] Luc Bousse, Piet Bergveld, "The Role Of Buried OH Sites In The Response Mechanism Of Inorganic-Gate pH-Sensitive ISFETs", *Sensors and Actuators*, vol. 6, pp. 65-78, 1984.

[17] S. Jamasb, S. D. Collins, and R. L. Smith, "A Physical Model for Threshold Voltage Instability in Si_3N_4-Gate H+-Sensitive FET'S (pH ISFET's)", *IEEE Transactions on Electron Devices*, vol. 45, no. 6, pp. 1239-1245, Jun, 1998.

[18] G. Pfister, H. Scher, "Time-dependent electrical transport in amorphous solid: As_2Se_3", *Physical Review B*, vol. 15, no. 4, pp. 2062-2082, Feb., 1977.

[19] H. Scher, Elliott W. Montroll, "Anomalous transit-time dispersion in amorphous solid", *Physical Review B*, vol. 12, no.6, pp. 2455-2477, Sep., 1975.

[20] J. Kakalios, R. A. Street, W. B. Jackson, "Stretched-Exponential Relaxation

Arising from Dispersive Diffusion of Hydrogen in Amorphous Sillicon", *Physical Review Letters*, vol. 59, no.9, pp. 1037-1040, Aug. 1987.

[21] S. Jamasb, S. D. Collins, R. L. Smith, "A Physically-based Model for Drift in Al_2O_3-gate pH ISFETs " in *International Conference on Solid-State Sensors and Actuators* Chicago, June, 1997.

[22] S. Jamasb, S. D. Collins, R. L. Smith, "A physical model for drift in pH ISFET ", *Sensors and Actuators B*, vol. 49, pp. 146-155, 1998.

Chapter 3

Experiment and Measurement

3.1 Introduction

The structure of ISFET is similar to the conventional MOSET. The most difference between MOSFET and ISFET is the gate electrode. The ISFET takes the gate membrane as a sensing layer immersed in the pH-solution [1]. In the experiment, we produce the n-type ISFET and the p-type ISFET. From the derivations of the ISFET sensitivity in chapter 2, there are no factors about electrons and holes. So we can guess that the sensitivity must be the same whether the substrate is n-type or p-type.

Besides the ISFET, we also produce the REFET. REFET is identical with ISFET except that REFET does not react on the ion concentration to be measured, i.e. REFET is insensitive to the test ion concentration [2]. We use the polymer materials coated on the ZrO_2 sensing layer to get the insensitive REFET. And then, we measure the electric parameters including the drift amount and the sensitivity of ISFET and REFET respectively.

3.2 The fabrication process flow of ISFET and REFET

The all procedures of experiment are accomplished in NDL (National Nano Device Laboratory) and NFC (Nano Facility Center). The fabrication process flow is shown in Fig. 3-1. And the detailed steps are listed in this section.

Part 1:

1. RCA clean.
2. Wet oxide growth 6000Å, 1050°C, 65mins.

Part 2:

3. Mask#1 for the definition of the regions of Source/Drain.
4. Wet etching of unblocked silicon dioxide.
5. Dry (Screening) oxide growth 300 Å, 1050°C, 12mins.
6. Source/Drain implantation:

   Dose= $5*10^{15}$ ($1/cm^2$), Energy= 15Kev (Boron) for p-type ISFET.

   Dose= $5*10^{15}$ ($1/cm^2$), Energy= 25Kev (Phosphorus) for n-type ISFET.

   The Above detailed information is in Table 3-1.
7. Source/Drain annealing, 950°C, 60mins.

Part 3:

8. PECVD Oxide deposition 1μm.

Part 4:

9. Mask#2 for the definition of the contact hole and gate region.
10. Wet etching of unblocked silicon dioxide.
11. Dry oxide growth 100 Å, 850°C, 60mins.

Part 5:

12. Mask#3 for the definition of the sensing layer region.
13. Sensing layer (ZrO_2) deposition by Sputtering 300 Å.
14. ZrO_2 sintering 600°C, 30mins.

Part 6:

15. Mak#4 to define the contact region.
16. Al deposition by sputtering 5000 Å.

Part 7:

17. Backside Al evaporation 5000 Å.

18. Al sintering 400°C, 30mins

Part 8:

19. Coating the polymer-based material as the REFET sensing layer.

3.3 The illustration of the core parts

In part 1, RCA clean is for the elimination of ions and clean for the silicon surface, to make the growing equality of Wet Oxide better.

In part 2, the area of the defined Source/Drain grow a layer of 100A screen oxide to protect the surface when ion-implantation. The other use of this layer of oxide is avoid the channeling effect while implantation. After ion-implantation, the doped ions with high energy destroy the structure of lattice sites of the silicon substrate, and repair it by the way of anneal.

In part 3, then using PECVD grow oxide 1 μm as insulation to prevent buffer solution effect the device when ISFET is immersed in the electrolyte.

In part 4, decide the gate oxide region, and then use BOE etching the unblocked oxide. It grows the better quality gate oxide100A with dry oxide.

In part 5, define the sensing layer region for growing 300A ZrO_2 cause its property of the high sensitivity, which is about 57mv/pH [3]. Table 3-2 is the sputtering parameters.

In part 6, deposition of 5000A Al for the defined electrode region.

In part 7, finished Backside Al evaporation 5000A is the primary process of ISFET.

In part 8, coating the polymer materials cause of its insensitivity onto the ISFET sensing layer.

Before step 19, we coat HMDS onto the ZrO_2 sensing layer to enhance the

adhesion of the interface between the ZrO_2 sensing layer and the insensitive polymer material.

In step 19, an important step in the process of REFET fabrication, we coat the polymer-based material onto the HMDS layer as the REFET sensing element. We use a three-layer structure to form the REFET sensing region. The HMDS and the specific polymer-based material are coated from bottom to top onto the ZrO_2 sensing layer. These materials conclude epoxy, the mix composition of phtoresistance (PR) and Nafion (NF), and the different ratio of the mixture of Nafion and polyimide (PI). The experiment test structures are listed in Table 3-3.

According to the data, Nafion (shown as Fig.3-2) is extremely resistant to chemical attack and able to be used in relatively high temperature, so Nafion can protect for the underlying layers from damaging. There is also an additional advantage for using Nafion. It is that Nafion is a cation exchange polymer, i.e. NFafion will not affect the hydrogen ions to pass and any sensitivity decreased. The coating procedure has to be controlled carefully, following is our process flow:

1. Prepare Epoxy, the mixture of NF and PR (FH6400) with the ratio of NF/PR = 1/1, the mixture of NF and PI with the ratio of NF/PI = 1/1 and 1/3, and the pure PI.
2. Dropping the above materials onto the HMDS above the ZrO_2 sensing layers. Dried in air for 30 hours, these materials become colloid with thickness of 5-10um.

3.4 Measurement system

3.4.1 Preparation before measurement

We obtain the I-V curves of the pH-ISFET from the measurement using HP4156 as measurement tool and the system (shown in Fig 3-3) to investigate the characteristics of the regular ISFETs and the REFET structures with the different polymer-based sensing layers. To reduce the disturbance from the environment, such as light influence, the entire measurement procedures were executed in a dark box [4]. The measured pH values are 1, 3, 5, 7, 9, 11, 13, and the pH buffer solution were supplied by the Riedel-deHaen corp.

3.4.2 The measurement of pH sensitivity

A HP-4156 semiconductor parameter analyzer system were set up to measure the *I-V* characteristic curves, in which include I_{DS}-V_{GS} and I_{DS}-V_{DS} curves at some specific controlled temperature. We must be careful while dropping the pH-buffer solution at the sensing region. Because of the small sensing areas, it could easily generate the air bubbles in the interface. Consequently, in order to measure in the more stable situation, we began to measure after about 30 seconds while the sensing layer getting immersed in the pH buffer solutions.

From I_{DS}-V_{GS} curves, we can extract the pH sensitivity (in the unit of mV/pH) of ZrO_2 pH-ISFET. First, we should decide the specific bias I_{DS} usually at the point of the maximum transconductance, i.e. the maximum slope of I_{DS}-V_{GS} curve. The sensitivity of pH-ISFET, the gate voltage difference between different pH value buffer solutions at the constraint of the chosen current I_{DS} in the I_{DS}-V_{GS} curve, is obtained. The illustration to find the selectivity is the sketched in Fig. 3-4.

3.4.3 The measurement of drift

To obtain the more accurate drift amount, we put the n-type and the p-type ISFETs respectively immersed in the buffer solution with pH 3, 5, 7, 9, 11 in the periods of 12 hours before measuring. Similarly, we put the REFETs into the pH 7 buffer solution in the period of 90 minutes before measuring. The REFET breaks easily so that we take the less immersion time. As the similar manner in measuring the selectivity, we can sketch the gate voltage versus time in 400 minutes with the equal intervals of 10 minutes. The illustration to find the drift is the sketched in Fig. 3-5.

3.5 References

[1] P. Bergvled,"Development of an ion-sensitive solid-state device for neurophysiological measurement", *IEEE Trans. On Bio-Med. Eng.* (1970) 70-71

[2] P. Bergveld, "Thirty years of ISFETOLOGY What happened in the past 30 years and what happen in the next 30 years", *Sensors and Actuators B*, vol. 88, pp. 1-20, 2003.

[3] K. M. Chang, K. Y. Chao, T. W. Chou, and C. T. Chang, "Characteristics of Zirconium Oxide Gate Ion-sensitive Field-Effect Transistors" *Japanese Journal of Applied Physics* Vol. 46 No. 7A pp. 4334-4338 2007.

[4] Paik-Kyun Shin, "The pH-sensing and light-induced drift properties of titanium dioxide thin films deposited by MOCVD", *Applied Surface Science*, vol. 214, pp. 214-221, 2003

Chapter 4

Results and Discussions

4.1 Introduction

The drift is an unavoidable phenomenon of pH-ISFETs, some studies already indicate that the gate voltage shift according to the immersed time goes on. It makes the inaccuracy of the output signal and the lower reliability. We will discuss the experiment results and propose a method to reduce the influence. In addition to drift, we also list the selectivity of p-type and n-type ISFET.

In section 4-2, the important properties of REFET such as the drift and the sensitivity are investigated. From the properties, we can choose the suitable inactive material as the REFET sensing layer.

4.2 The p-type and n-type ISFET

We choose ZrO_2 as a sensing film of pH-ISFET for the reason of the higher sensitivity. Fig. 4-1 and Fig. 4-2 individually represent the measured I_{DS}-V_{GS} curves from pH 1 to pH 13 of the p-type and the n-type pH-ISFETs. The sensitivity is 57.8 mV/pH for the p-type ISFET and 58.73 mV/ pH for the n-type ISFET. The bias conditions of the two ISFETs are all arranged in Table 4-1. The high sensitive ZrO_2 gate ISFET in the readout circuits could accomplish the high revolution while determining the pH value. Besides of the higher sensitivity, the ZrO_2 film also includes other advantages [1].

Additionally, we focus on the drift phenomenon of the p-type and the n-type

ZrO_2 pH-ISFET. According to Ref. 2, we know the drift phenomenon is a complex function with the variables such as containing time, sensing film quality and pH aqueous solution. In order to obtain the more precise experiment results, the time and the film must be controlled at same condition in the different pH aqueous solutions. Fig. 4-3 ~ 4-7 are the gate voltage with times for 400 minutes drift in the intervals of equal 10 minutes to the pH 3, 5, 7, 9, 11 aqueous solution of p-type ISFET. Similarly, Fig. 4-8 ~ 4-12 show times for 400 hours drift in the pH 3, 5, 7, 9, 11 aqueous solution of n-type ISFET. From these results, we can find that the drift is a time dependent function which is obeyed with the study investigated by S. Jamasb [3]. The model presented by hydration S. Jamasb indicates that the hydration is a continuous process. The immersion in the solutions only diminishes the drift amount. The action can not vanish the phenomenon.

We also find that the drift phenomenon is related with the pH aqueous solution from Fig. 4-13 and Fig. 4-14. The drift comparison between p-type ISFET and n-type ISFET are listed in Fig. 4-15 and Fig. 4-16. The drift rate increasing with pH value is obeyed with prior research [4]. From our measurements, the direct proportion between the drift rate and the pH value almost exists no matter the categories of ISFET. The possible mechanism of the result is discussed in the following. OH^- plays a major role in the hydration action. In the alkali solutions, the more hydroxyl ions make the hydration more. So the drift rates increase with pH value.

From the experiment results, a possible method is proposed to reduce the drift influence at the region of pH 5 – pH 11. In the n-type ISFET, we define the real gate voltage $\boldsymbol{N} = n - \Delta n$. n represents the gate voltage of the ideal n-type ISFET, and $-\Delta n$ is the drift amount of the n-type ISFET. We can know that n and Δn are both positive numbers. So the signal to noise ratio is indicated as $S/N|_{\text{n-type ISFET}} = n/\Delta n$. In the p-type ISFET, we can similarly find the $S/N|_{\text{p-type ISFET}} = p/\Delta p$. p and Δp are both

positive numbers. To reduce the drift effect, we can define a new variable $\boldsymbol{T} = \boldsymbol{N} - \boldsymbol{P}$. From the above discussions, we can find $\boldsymbol{T} = (n+p) - (\Delta n - \Delta p)$. And then the S/N ratio is calculated as $S/N|_T = n + p/\Delta n - \Delta p$. By comparing the three S/N ratios, we know that $S/N|_T$ is larger than $S/N|_{\text{n-type ISFET}}$ and $S/N|_{\text{p-type ISFET}}$. The comparison between the original S/N and the modified S/N is listed in Table 4-2. From Table.4-2, the proposed method can enhance the S/N ratio. In other words, we can reduce the drift influence with the introduction of the new variable $\boldsymbol{T}$.

4.3 The results in the REFET structure

We coat the HMDS film to improve the adhesion between the ZrO_2 layer and the selected materials. Because of the focus is other materials in this experiment, we do not hope the additional function provided from HMDS. Fig. 4-17 is the selectivity of the structure of HMDS/ZrO_2. It shows that HMDS is not the major factor in the reduction of the sensitivity. The transconductance comparison between the ZrO_2 layer and the HMDS/ZrO_2 structure is shown in Fig. 4-18. The transconductances are almost the same. From Fig. 4-17 and Fig. 4-18, HMDS is an acceptable choice for improving the adhesion.

The parameter, transconductance (g_m), is an important property for the decision whether a material was chosen as the REFET sensing layer. It is troublesome to design two different circuits to maintain the reference bias point if the transconductance of the specific material is not similar with that of the ZrO_2 gate ISFET. The second reason for the same transconductance is the essentiality to select the REFET material. REFET is identical with ISFET except the low pH sensitivity. Usually, we take ISFET and REFET to combine together with a differential OP amplifier. The output signal is only associated with the pH value after the elimination

of the common mode signal of the differential OP amplifier. If the transconductance is extremely different, the output voltage is related with many factors. Therefore, the transconductance of materials is an essential factor which can help us to make an appropriate decision.

At the beginning of this experiment, we investigated epoxy, the mix composition of photoresistant (PR) and Nafion (NF) and the mixture of polyimide (PI) and Nafion. Fig. 4-19 shows the comparison of their transconductances. Fig. 4-19 implies that epoxy is not suitable in the situation. We can only use the two mixtures. Because of the better reliability (the smaller drift rate, show as Table 4-3), we choose the mixture of Nafion and polyimide finally.

We find the variation in transconductance compared with the original ZrO_2 sensing layer when we choose the different sensing materials [5]. Therefore, we are interested in the composition of this structure. We tried to change the proportion of Nafion compared to polyimide. Consequently, the pure polyimide and 1/1, 1/3 ratios of Nafion/polyimide are treated as the possible adoptable implements. These characteristics are discussed in the next paragraph.

The six figures, from Fig. 4-22 to Fig. 4-27, are the results of our measurements. For the convenience, we arrange these experimental results in Table 4-4. Certainly, their transconductances are compared in Fig. 4-28. We can identify that the amount of Nafion affect. Nafion is a cation exchange polymer, so the more Nafion brought out the higher sensitivity. But a lower sensitivity is needed to form a REFET structure. Less Nafion make the lower sensitivity. It can make the better drift rate because of the better adhesion at the same time. To reduce the amount of Nafion seems that a good method to achieve the goal to find the suitable material. However, the larger shift in transconductance in this situation shown in Fig. 4-28. The pure polyimide acts like the ion blocking material, such as epoxy. Therefore, there is a trade-off in formulating the

suitable ratio of the mixture of the polymer based sensing material.

4.4 Conclusions

In the first part, we know that the ZrO_2 gate ISFET is a good choice for circuit design because of its high sensitivity. The high sensitivity could provide the high resolution. The sensitivity is 57.08 mV/pH for the p-type ISFET and 58.73 mV/pH for the n-type ISFET. Fig. 4-15 and Fig. 4-16 are the figures of the amount and the rate of drift. We can reduce the drift influence by introducing a new variable $\boldsymbol{T = N - P}$. $\boldsymbol{N}$ and $\boldsymbol{P}$ respectively represent the gate output voltage.

In the second part, we find the modulation of the compositions of the polymer based material can obtain good properties. In this situation, the 1/1 ratio of Nafion/polyimide is the better choice. From Table 4-4 and Fig. 4-28, the behavior of this structure is almost the same as ZrO_2 film, and its sensitivity and drift rate are the acceptable quantities. Although the best selectivity and the drift are the pure polyimide, it is inconsistent with the ZrO_2 film in the part of transconductance. We may increase the complexity of readout circuits if we use the pure polyimide as the sensing material. In this situation, it is difficult to produce the small size sensors. To select the similar material in transconductance is the significant consideration for the commercial applications.

4.5 References

[1] K. M. Chang, K. Y. Chao, T. W. Chou, and C. T. Chang, ”Characteristics of Zirconium Oxide Gate Ion-sensitive Field-Effect Transistors” *Japanese Journal of Applied Physics* Vol. 46 No. 7A pp. 4334-4338 2007.

[2] S. Jamasb, S. D. Collins, R. L. Smith, ”A Physically-based Model for Drift in Al_2O_3-gate pH ISFETs ” in *International Conference on Solid-State Sensors and Actuators* Chicago, June, 1997.

[3] S. Jamasb, S. D. Collins, and R. L. Smith, ”A Physical Model for ThresholdVoltage Instability in Si_3N_4-Gate H+-Sensitive FET’S (pH ISFET’s)”, *IEEE Transactions on Electron Devices*, vol. 45, no. 6, pp. 1239-1245, Jun, 1998.

[4] J. C. Chou, Y. F. Wang, ”Preparation and study on the drift and hysteresis properties of the tin oxide gate ISFET by the sol-gel method”, *Sensors and Actuators B*, vol.86, pp. 58-62, 2002.

[5] C. S. Lai, C. E. Lue, C. M. Yang, M. Dawgul, and D. G. Pijanowska, “Optimization of a PVC Membrane for Reference Field Effect Transistors”, *Sensors*, vol. 9, pp. 2076-2087, 2009.

Chapter 5

Future Work

Among this experiment, we propose a method to reduce the effect of drift. We also find the specific composition of the mixture of polyimide and nafion as the suitable REFET sensing layer material. To realize simplified compensation and readout circuits with matched transconductance for ISFET/REFET pair is the future objective.

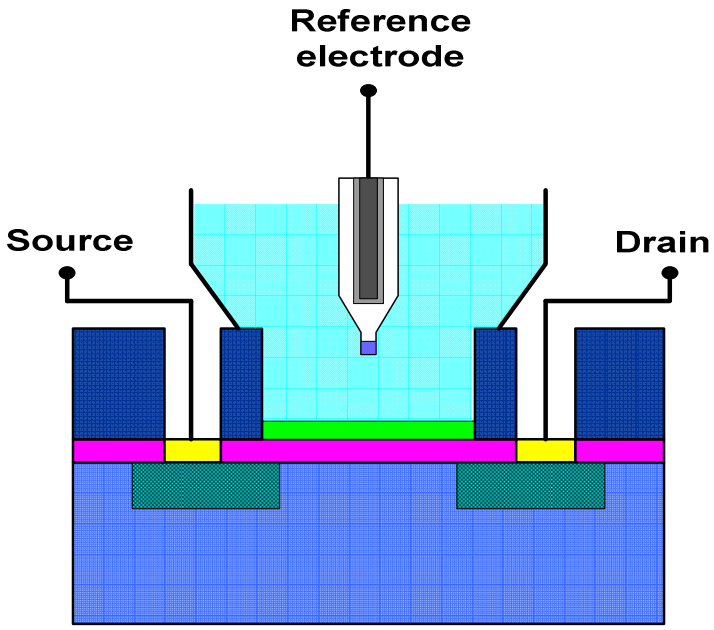

Fig. 1-1 ISFET cross-section structure

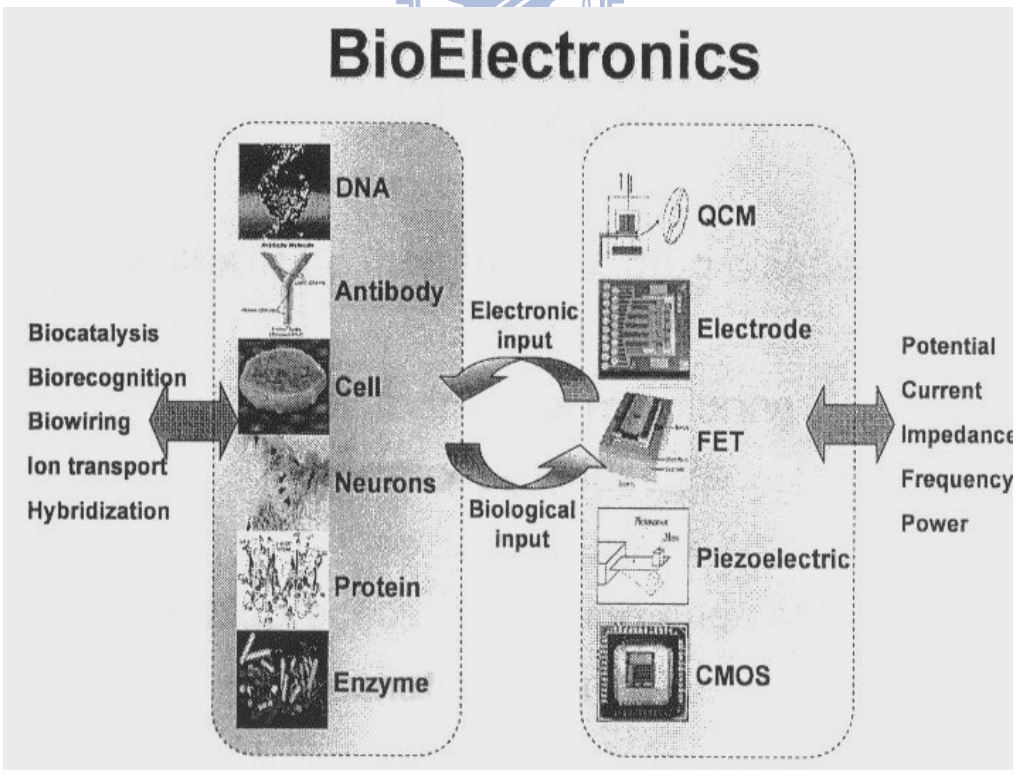

Fig. 1-2 Important platform of Bio-sensors

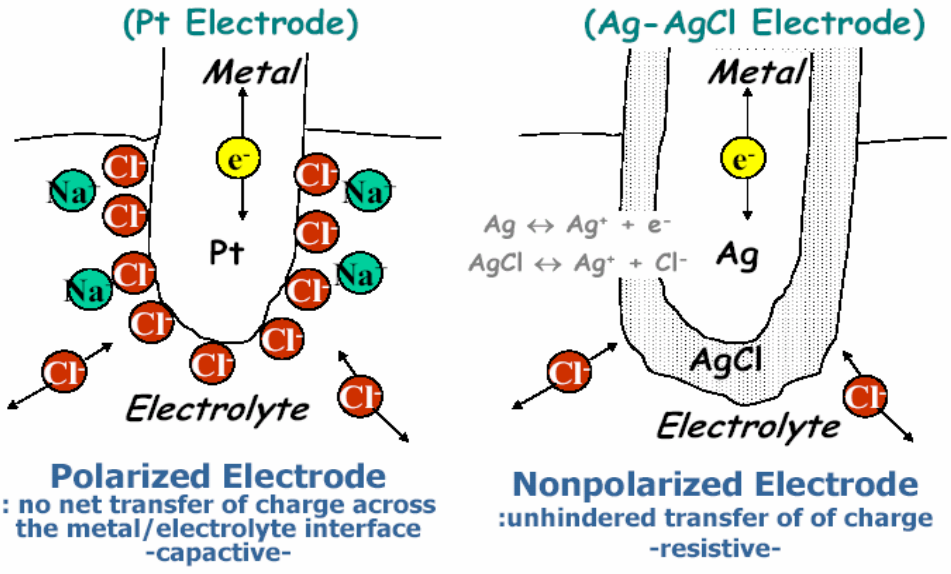

Fig. 1-3 The electrode structures

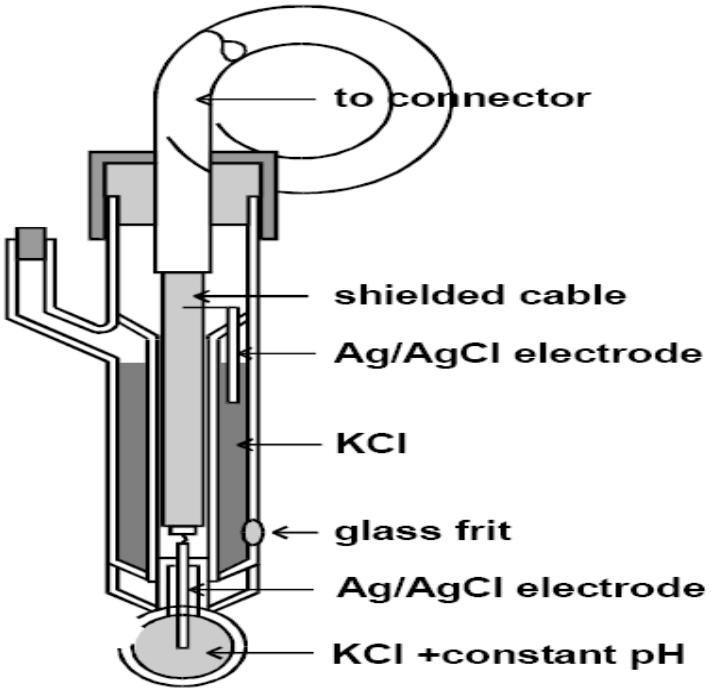

Fig. 1-4 Conventional glass electrode

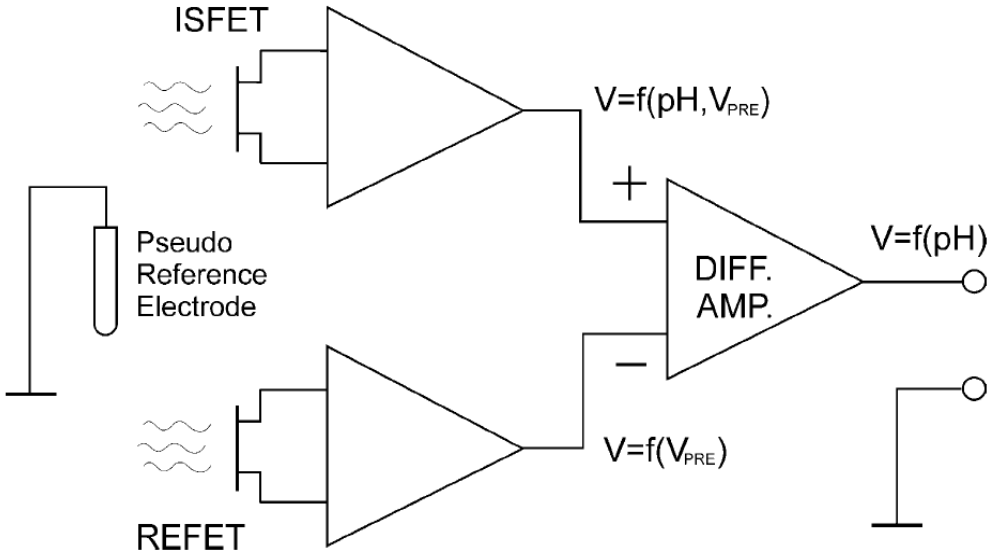

Fig. 1-5 Differential ISFET/REFET measuring system

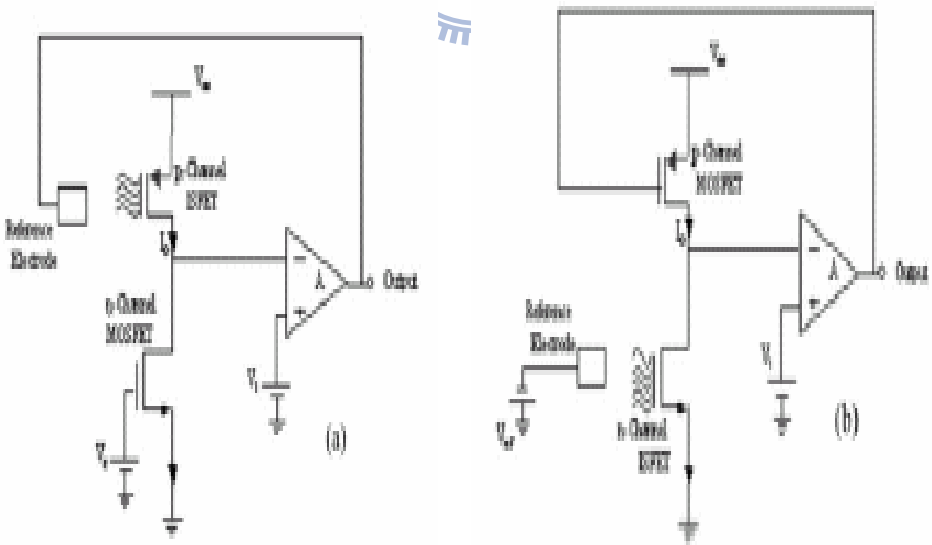

Fig. 1-6 Direct (a) and indirect (b) feedback circuit

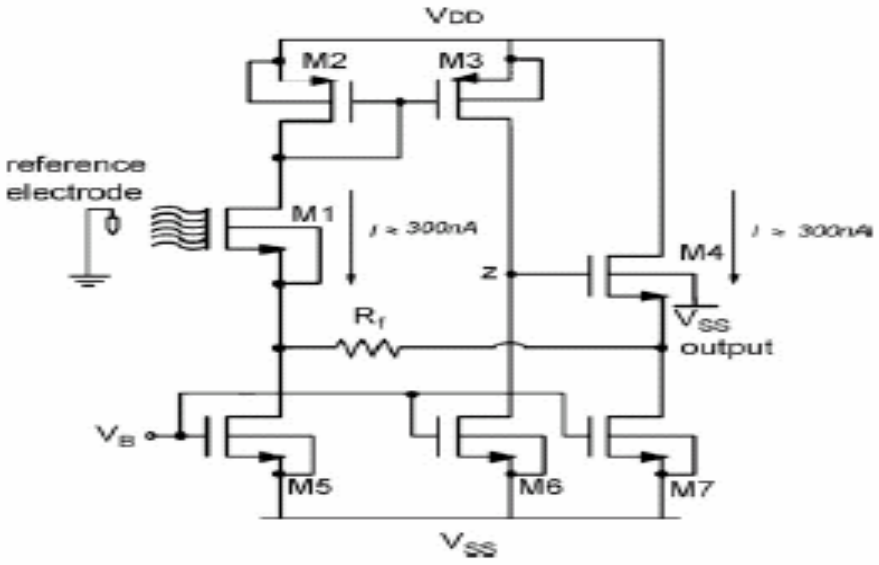

Fig. 1-7 Sketch of readout circuit with global feedback

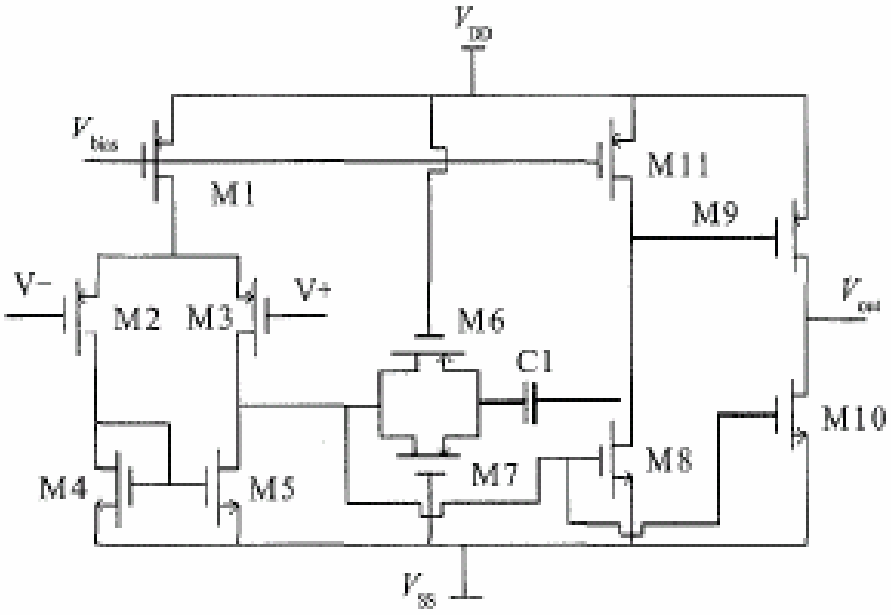

Fig. 1-8 Sketch of an operational amplifier

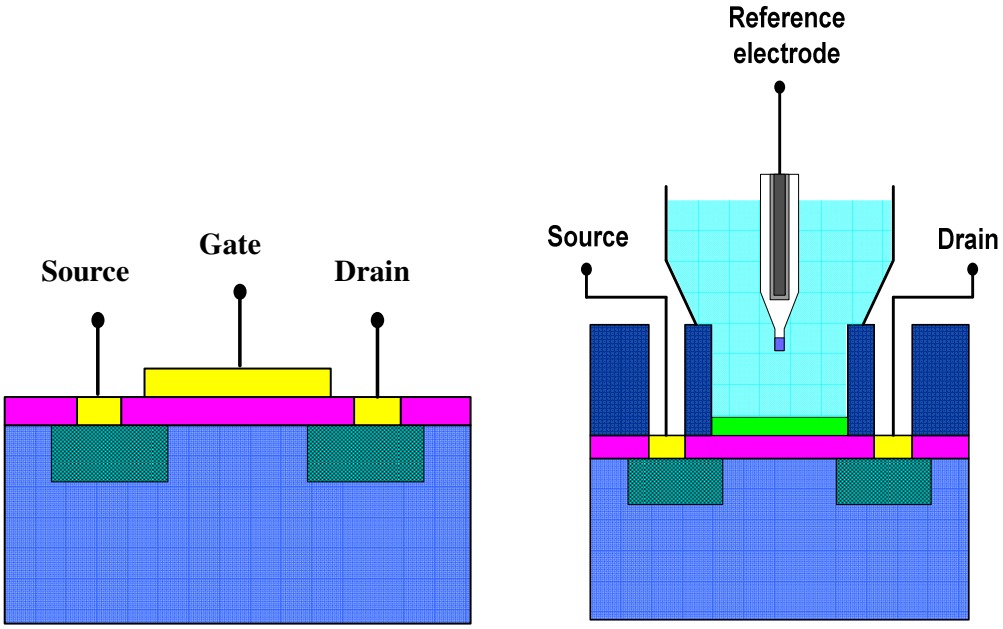

Fig. 2-1 Structure of MOSFET and ISFET

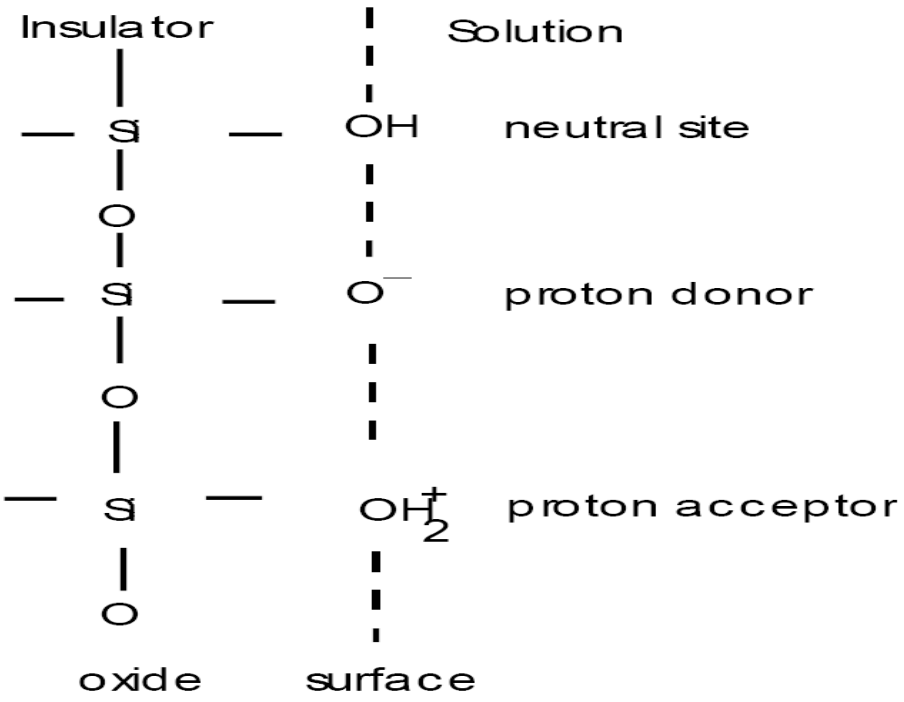

Fig. 2-2 Site-binding model

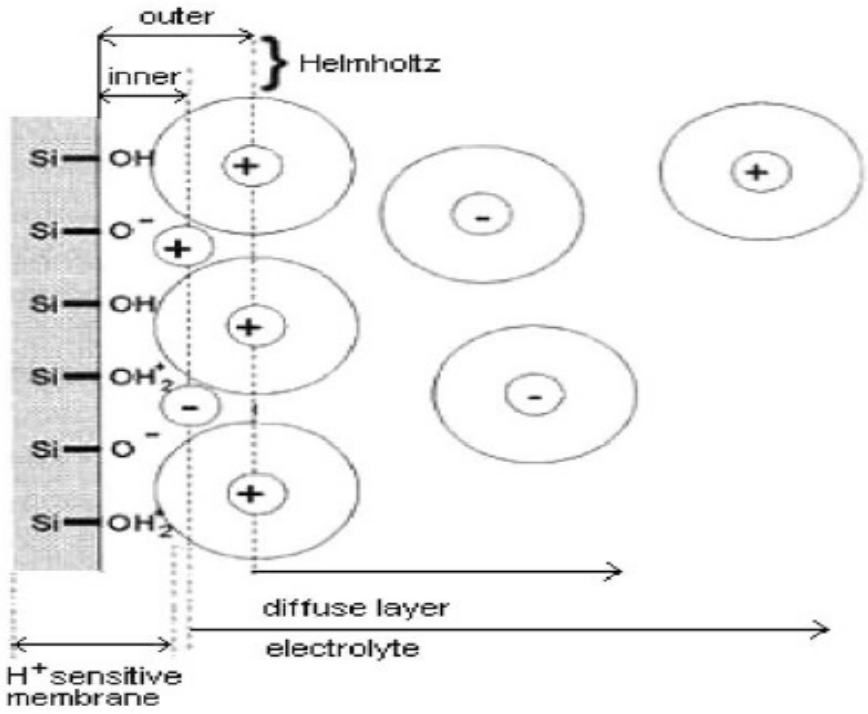

Fig. 2-3 The interface between silicon dioxide and electrolyte

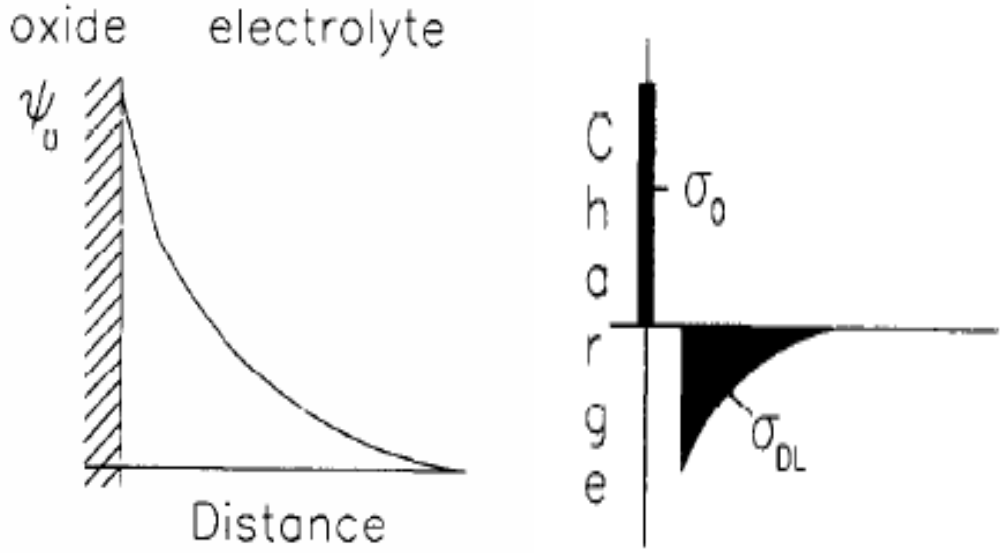

Fig. 2-4 Potential profile and charge distribution at an oxide electrolyte solution interface

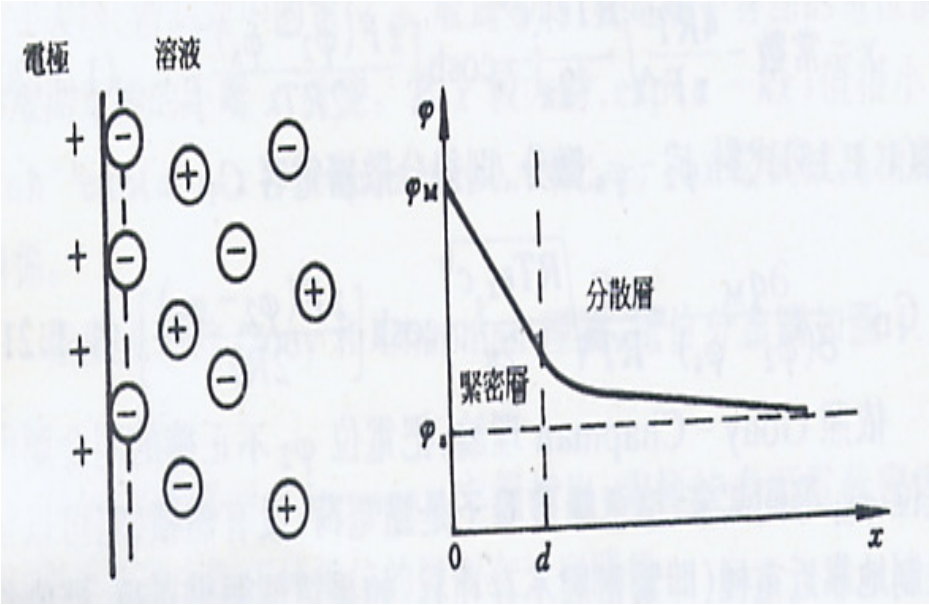

Fig. 2-5 Gouy-Chapman-Stern model

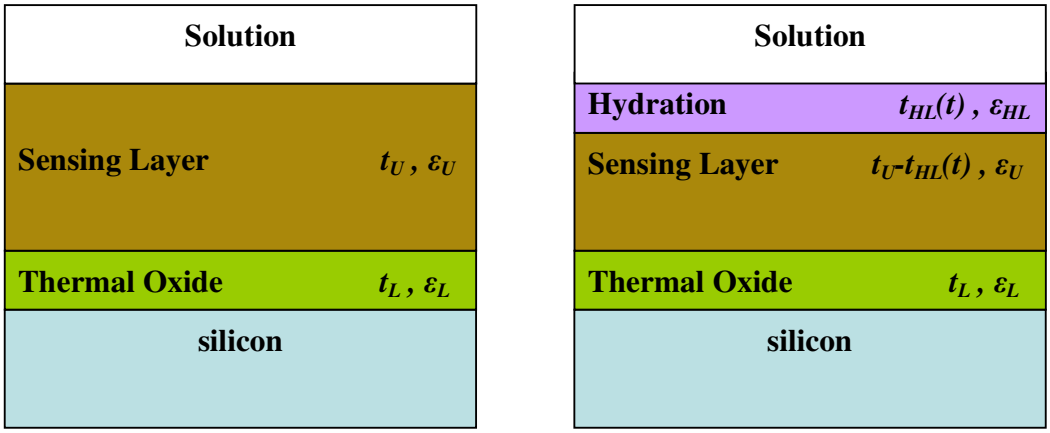

Fig. 2-6 Series combination of the (a) initial (b) hydrated insulator capacitance

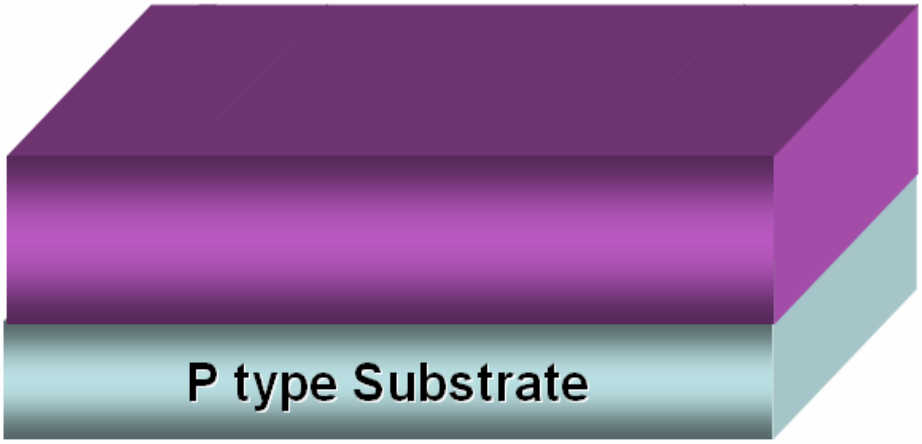

Part 1

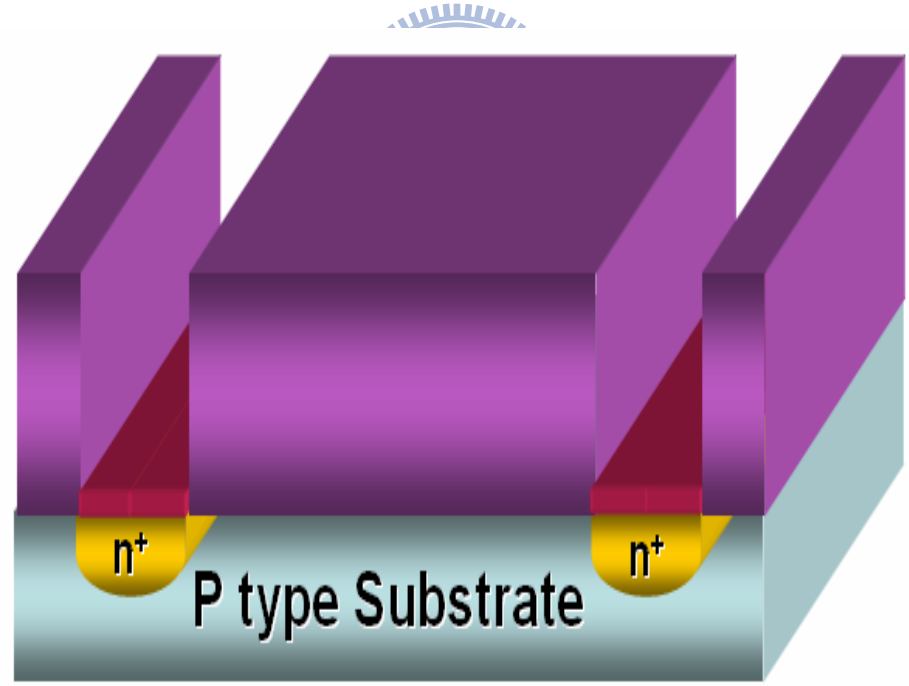

Part 2

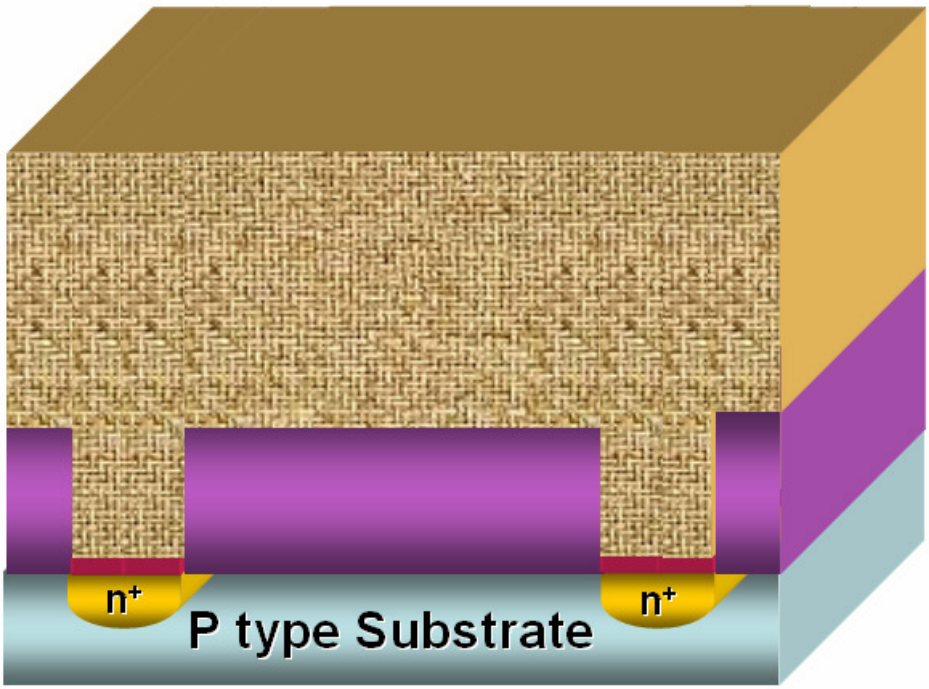

Part 3

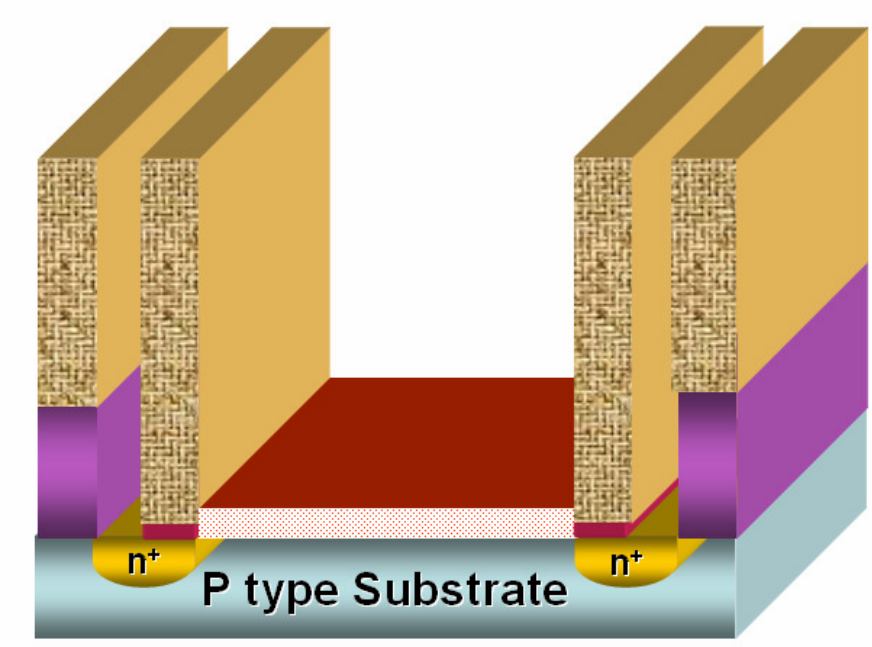

Part 4

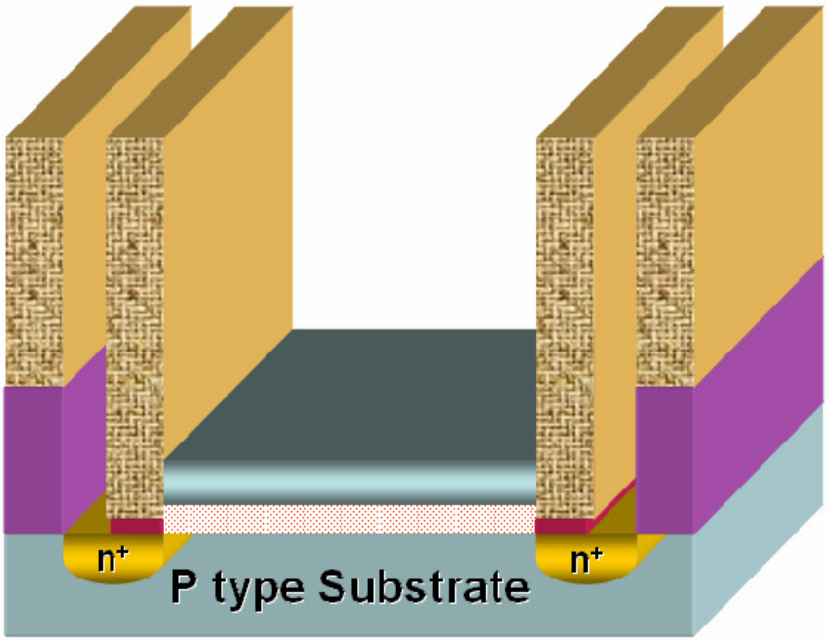

Part 5

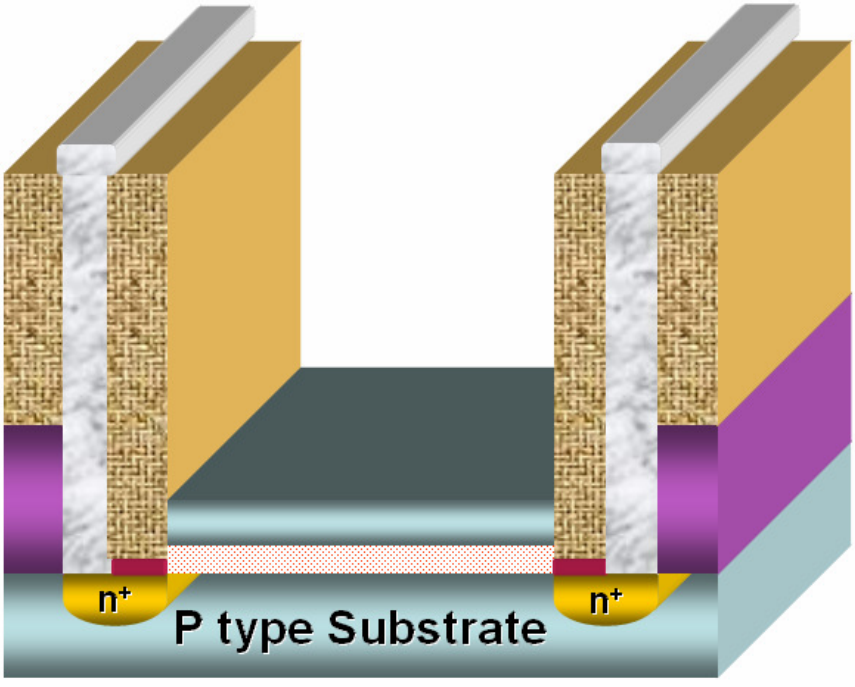

Part 6

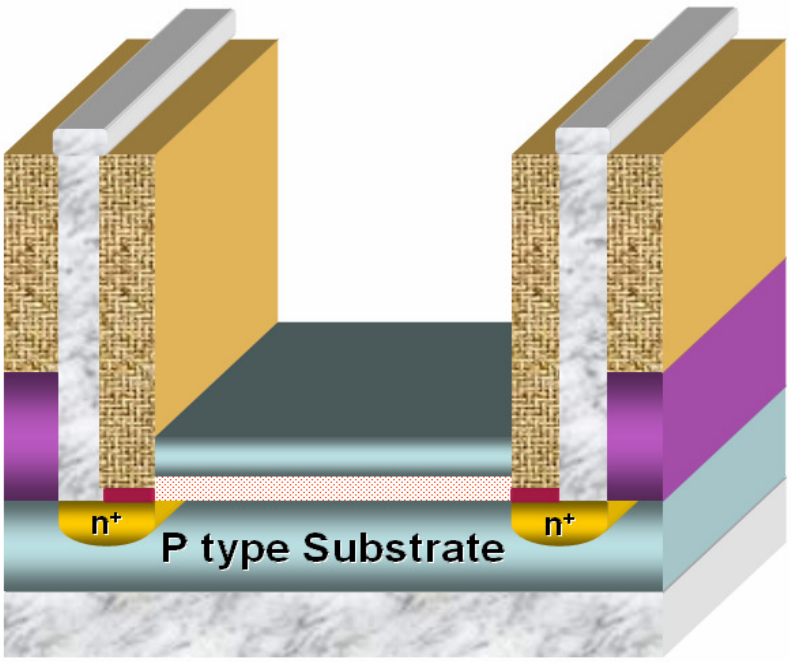

Part 7

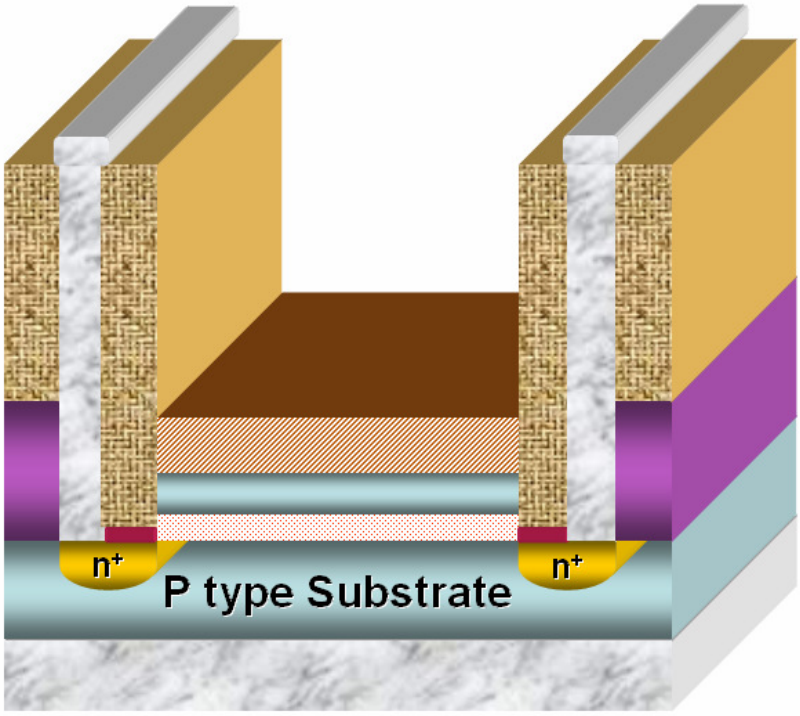

Part 8

Fig. 3-1 Fabrication process flow

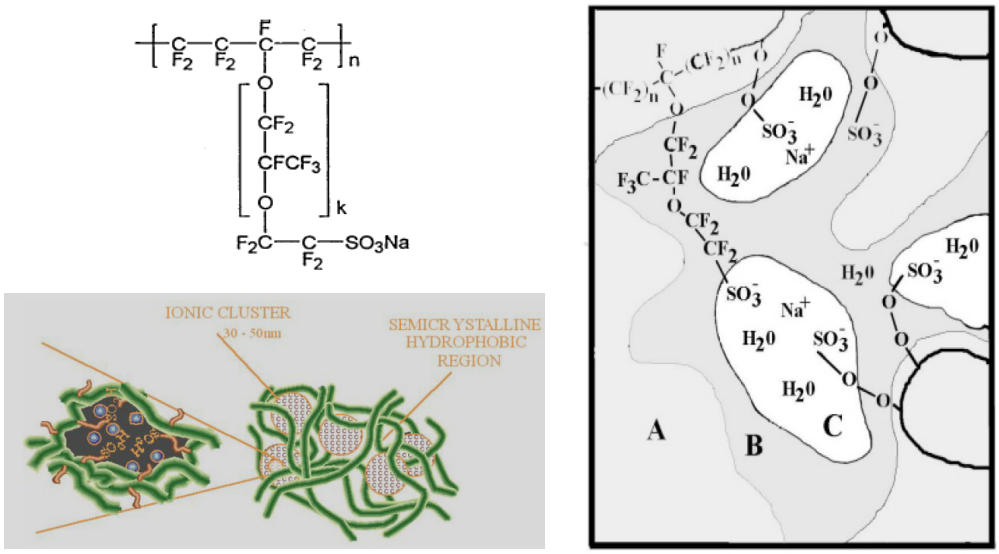

Fig. 3-2 Chemical formula and sketch for Nafion

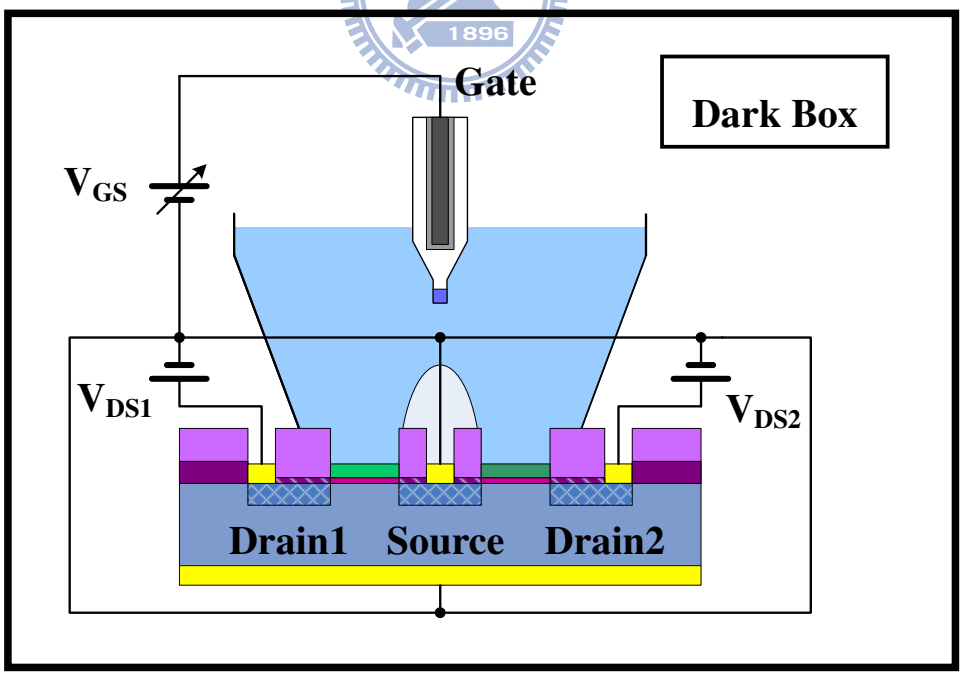

Fig. 3-3 Measurement set-up

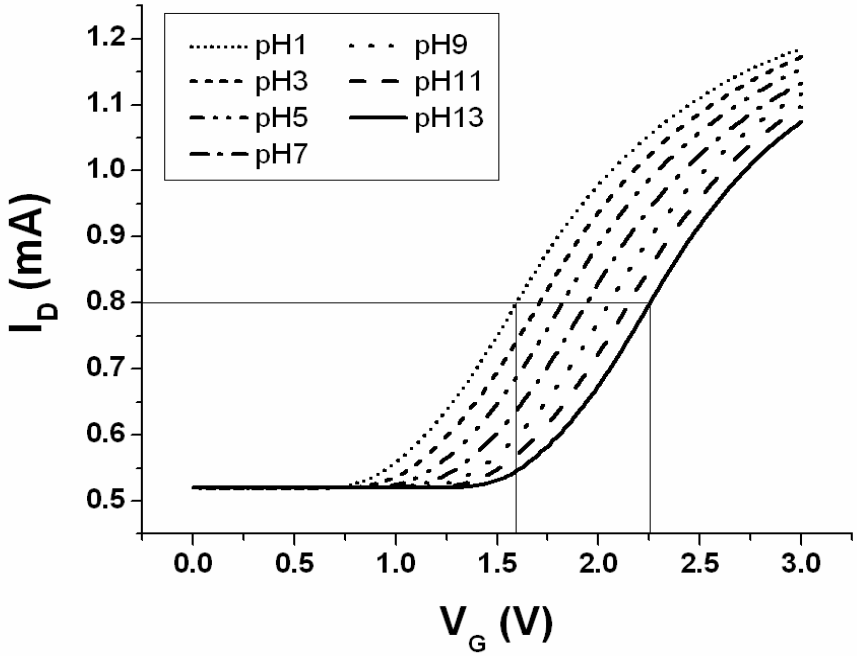

Fig. 3-4 Detection principle of pH

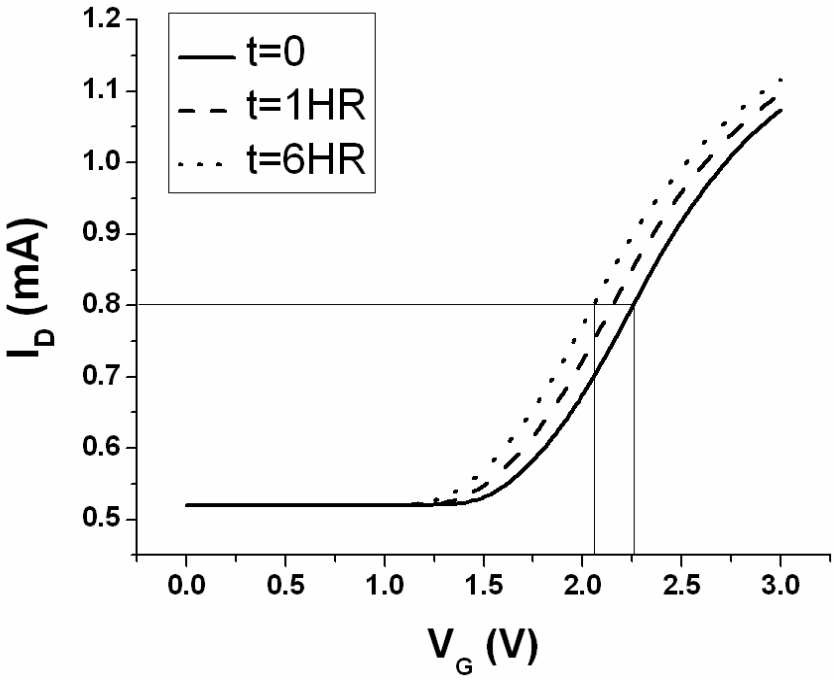

Fig. 3-5 Detection principle of drift

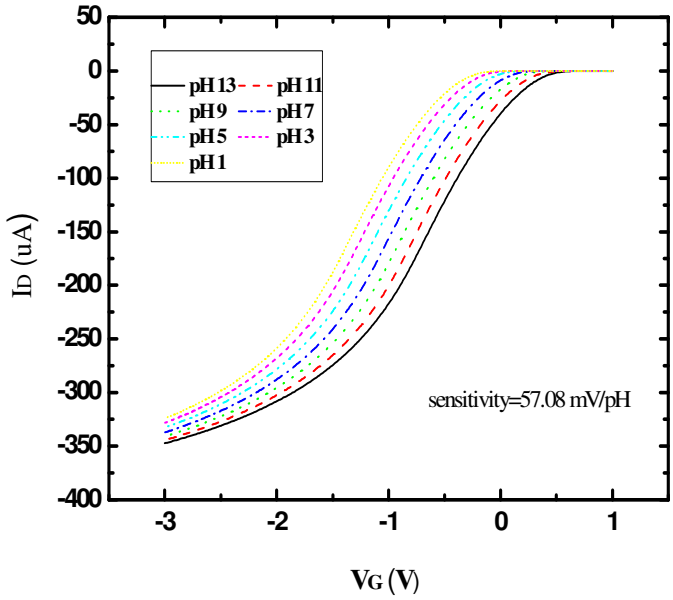

Fig. 4-1 Id-Vg curve of ZrO_2 for p-type ISFET before drift

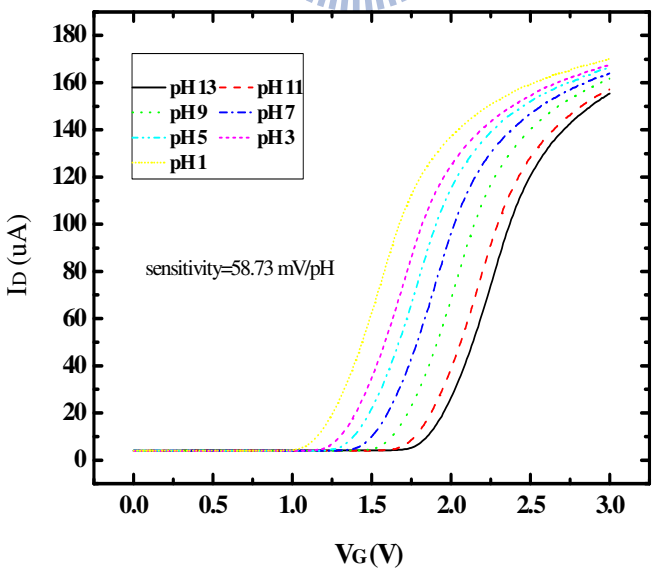

Fig. 4-2 Id-Vg curve of ZrO_2 for n-type ISFET before drift

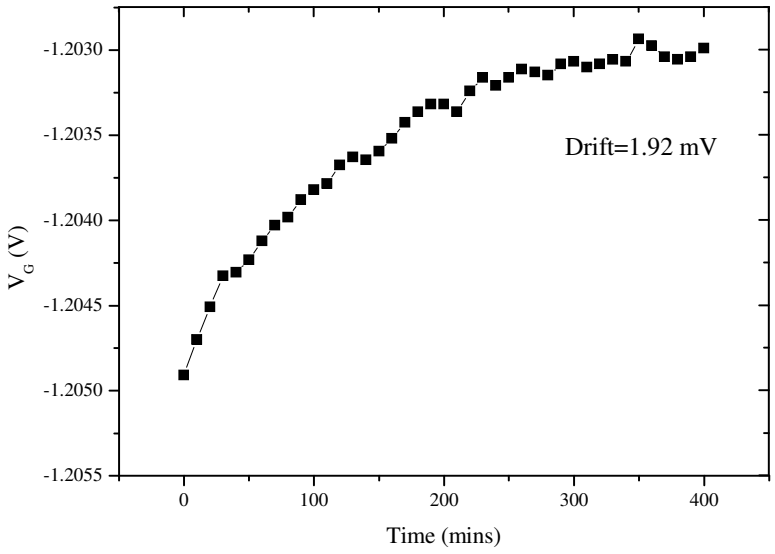

Fig. 4-3 Time to drift in pH 3 buffer solution of p-type ISFEET for 400 minutes

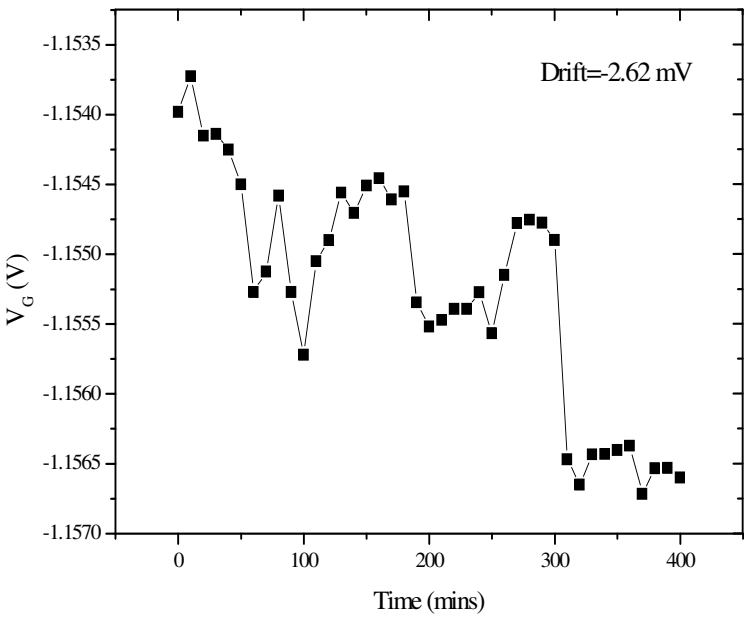

Fig. 4-4 Time to drift in pH 5 buffer solution of p-type ISFEET for 400 minutes

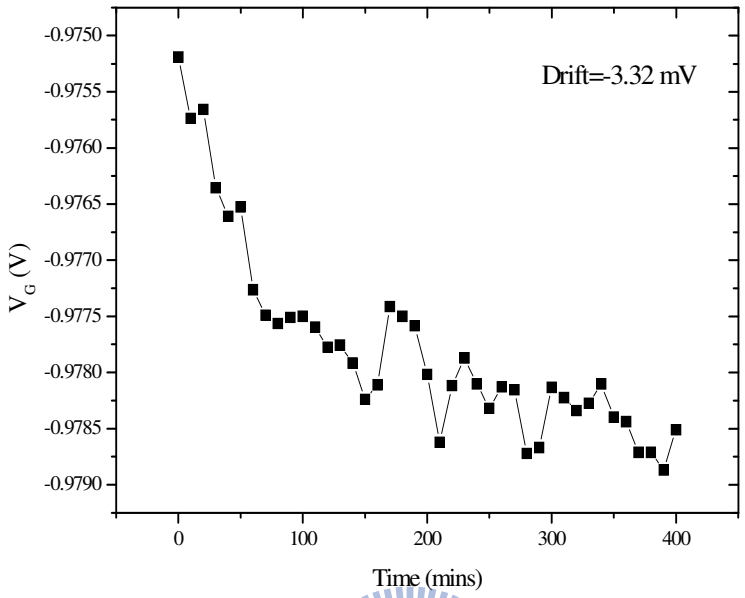

Fig. 4-5 Time to drift in pH 7 buffer solution of p-type ISFEET for 400 minutes

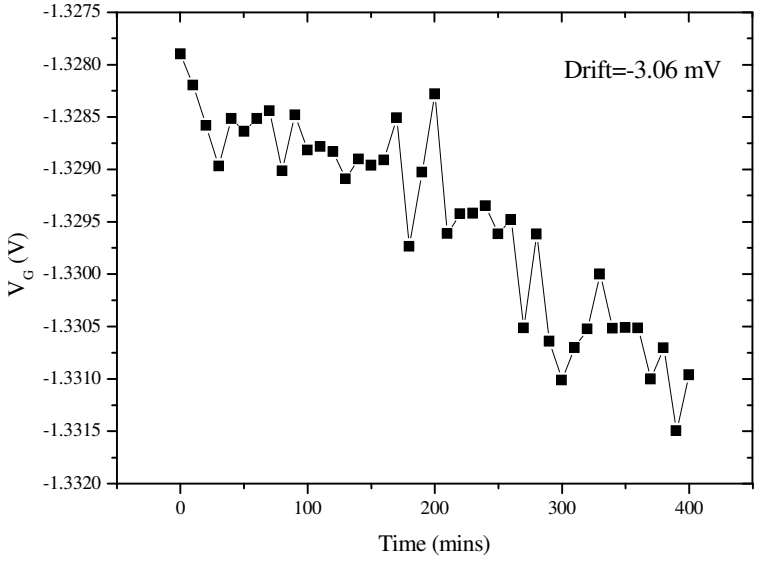

Fig. 4-6 Time to drift in pH 9 buffer solution of p-type ISFEET for 400 minutes

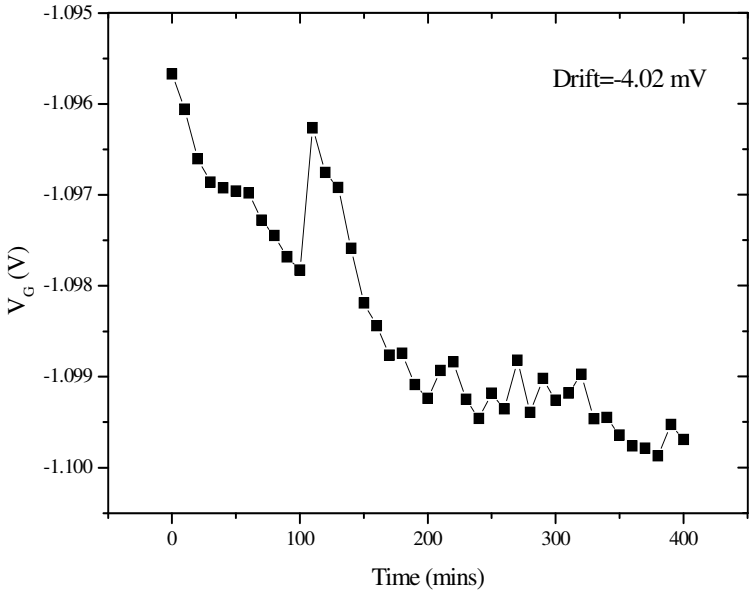

Fig. 4-7 Time to drift in pH 11 buffer solution of p-type ISFEET for 400 minutes

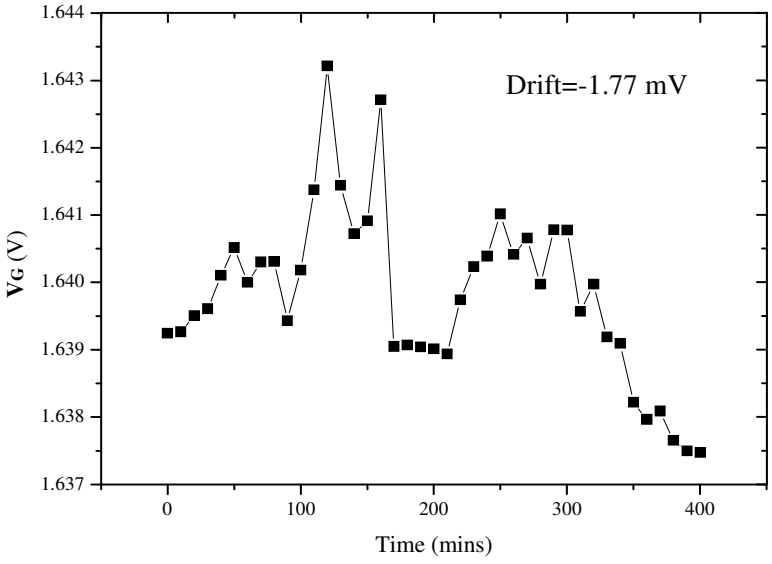

Fig. 4-8 Time to drift in pH 3 buffer solution of n-type ISFEET for 400 minutes

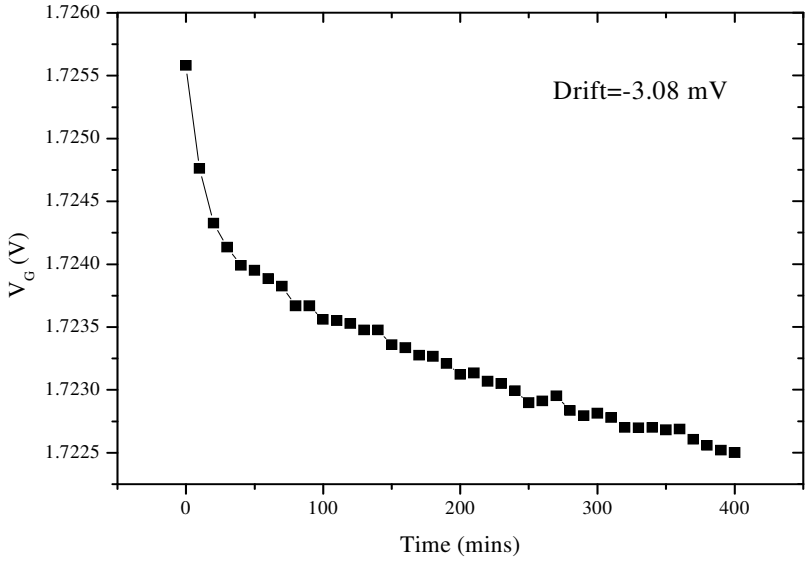

Fig. 4-9 Time to drift in pH 5 buffer solution of n-type ISFEET for 400 minutes

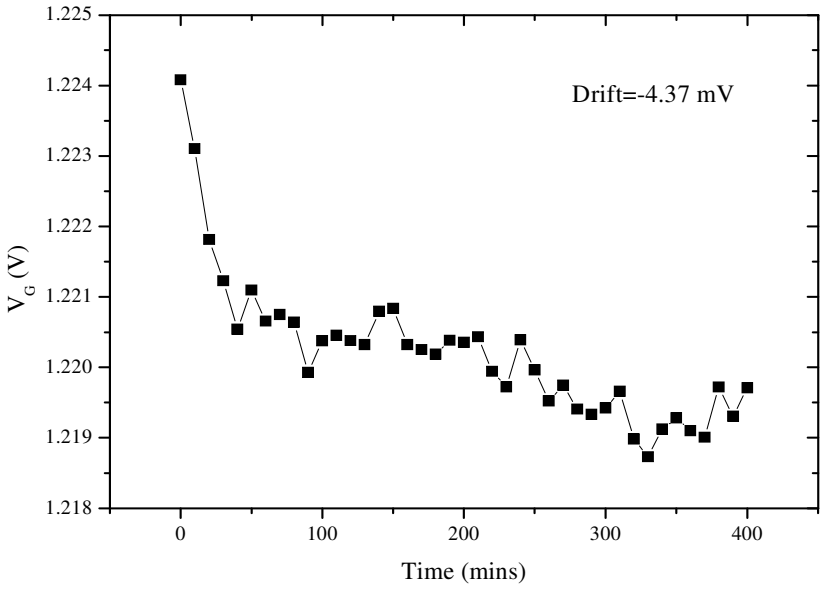

Fig. 4-10 Time to drift in pH 7 buffer solution of n-type ISFEET for 400 minutes

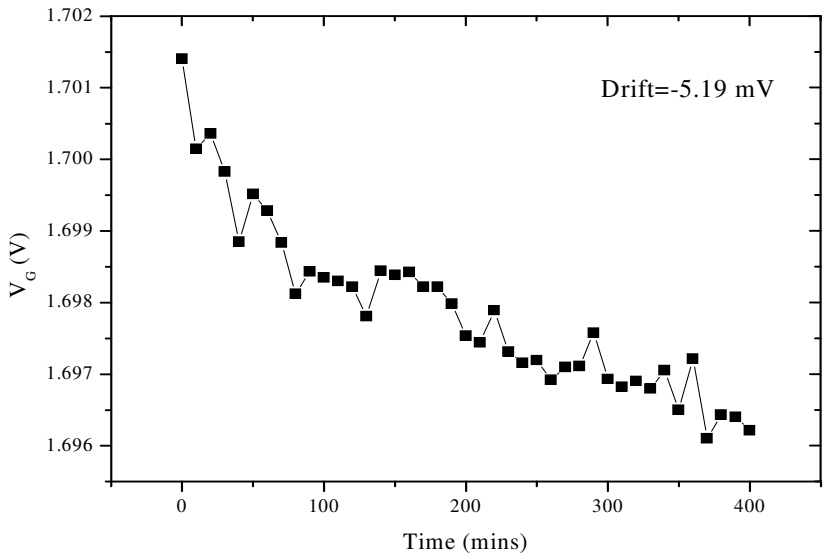

Fig. 4-11 Time to drift in pH 9 buffer solution of n-type ISFEET for 400 minutes

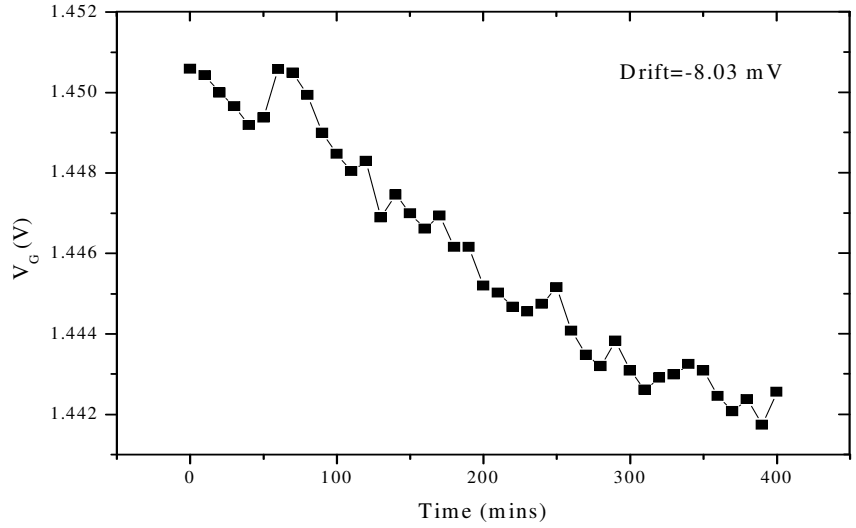

Fig. 4-12 Time to drift in pH 11 buffer solution of n-type ISFEET for 400 minutes

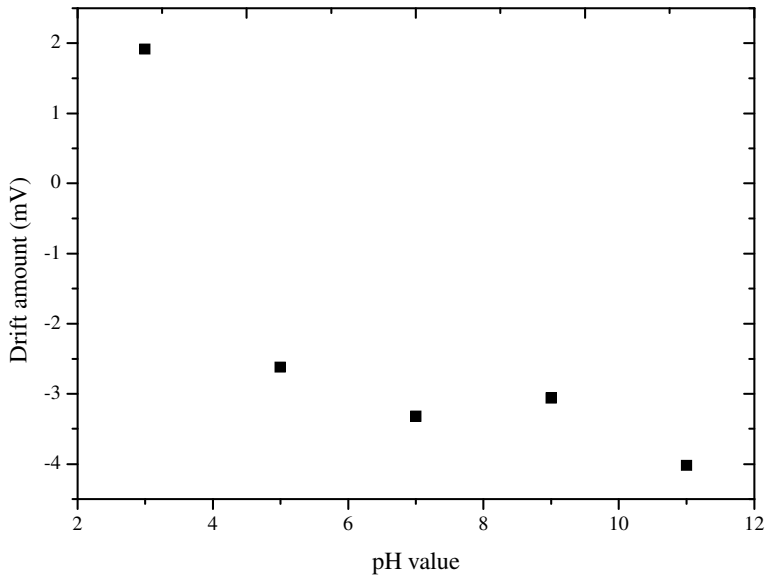

Fig. 4-13 Time to drift rate of p-type ISFET in various buffer solution

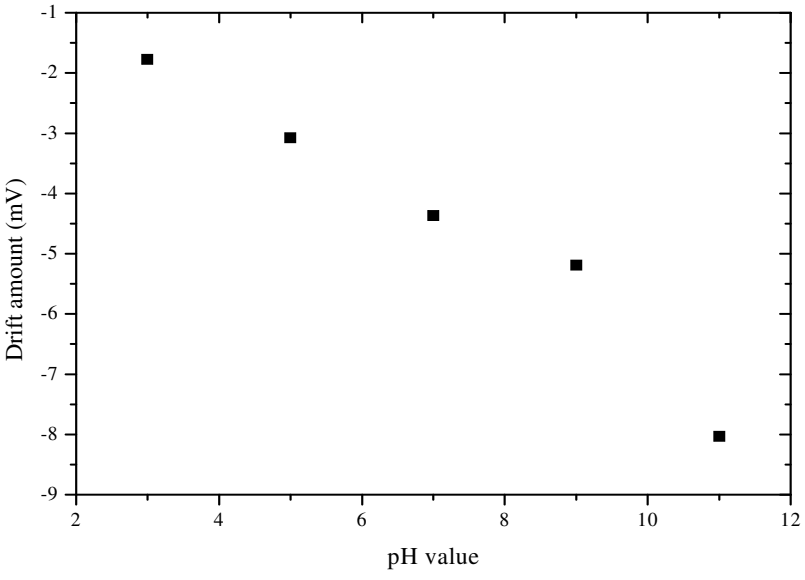

Fig. 4-14 Time to drift rate of n-type ISFET in various buffer solution

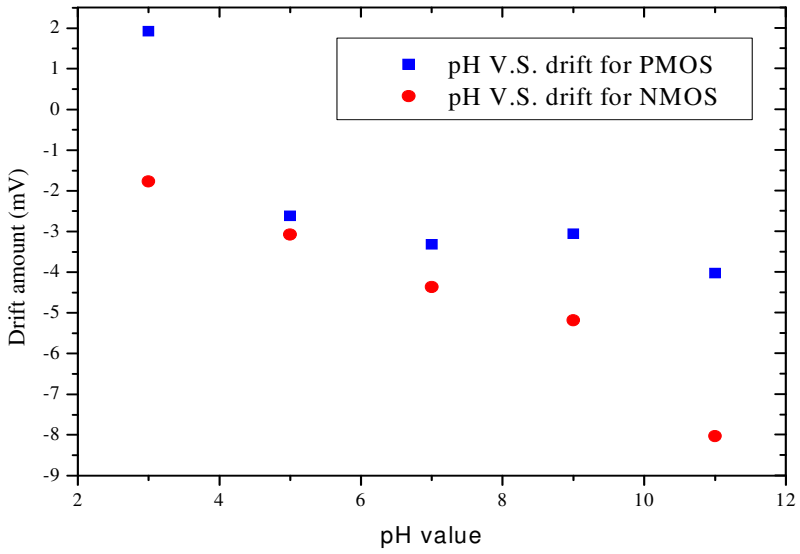

Fig. 4-15 Comparison of drift amount between p-type and n-type ISFET in various buffer solutions

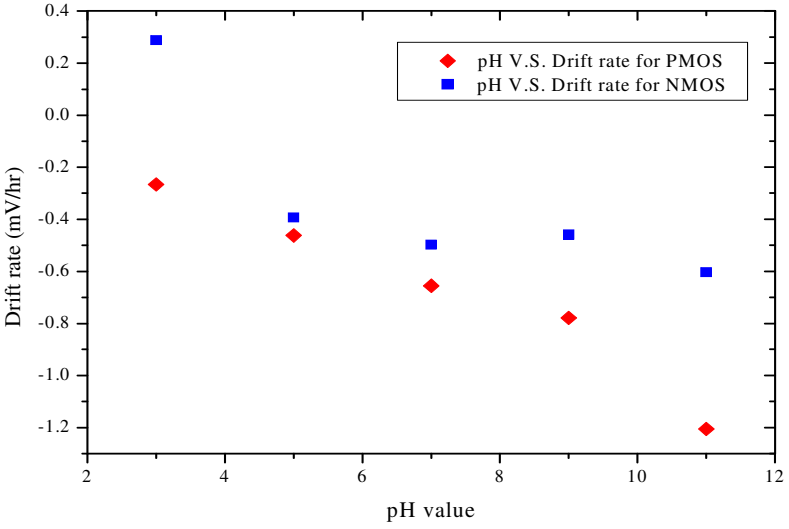

Fig. 4-16 Comparison of drift rate between p-type and n-type ISFET in various buffer solutions

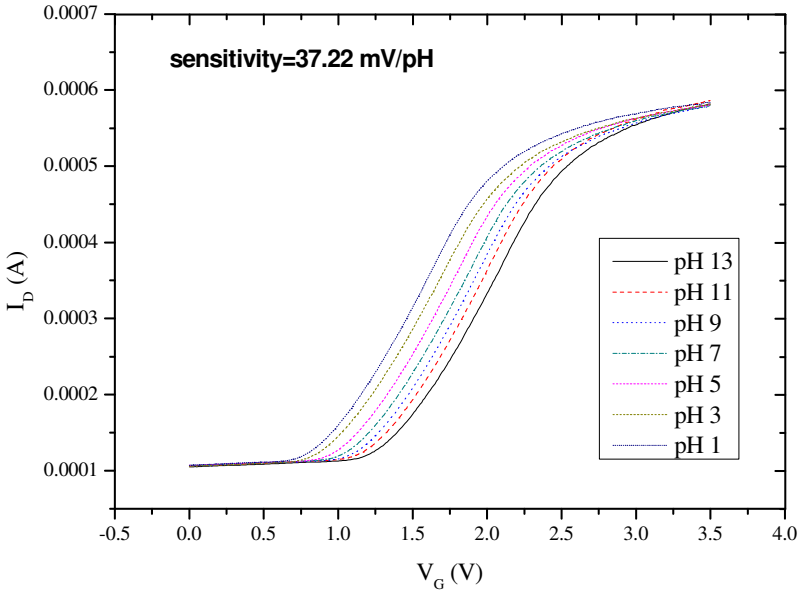

Fig. 4-17 Selectivity of the HMDS/ZrO_2 structure

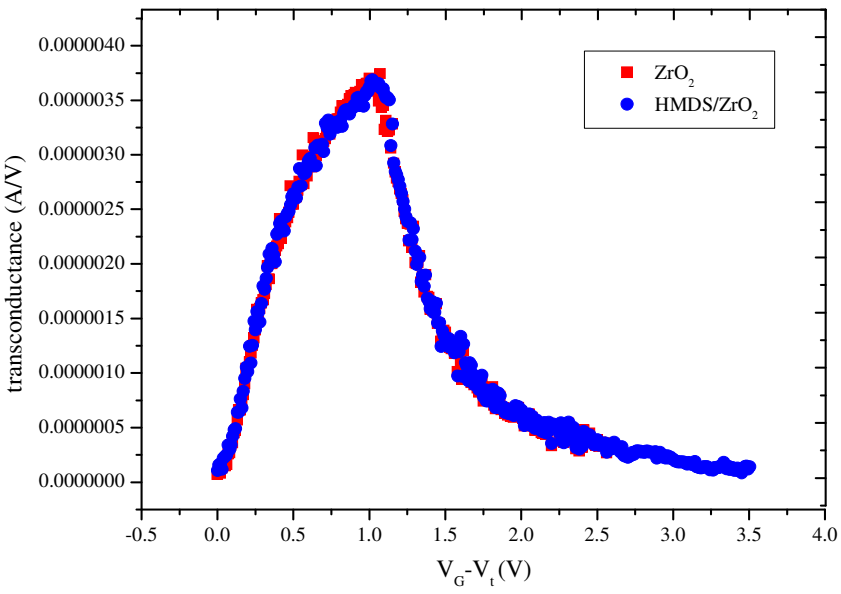

Fig. 4-18 Comparison of g_m between ZrO_2 and the HMDS/ZrO_2 structure

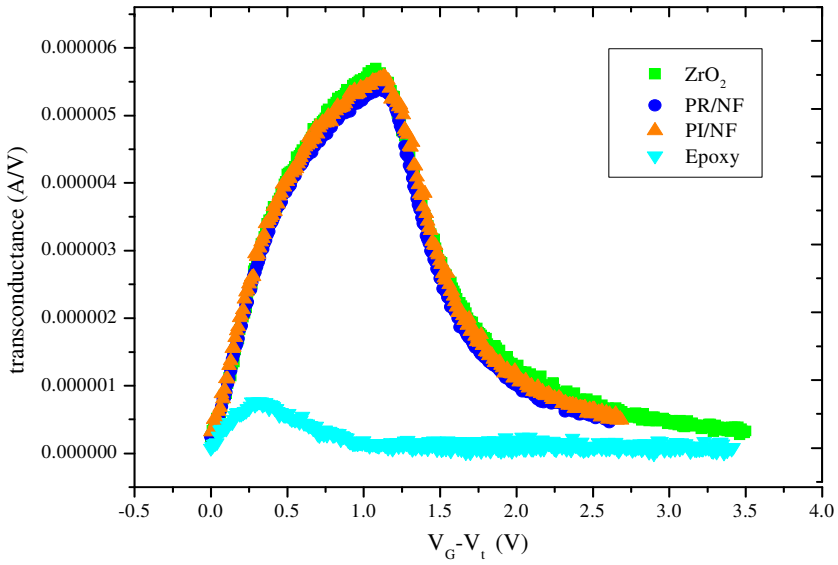

Fig. 4-19 Comparison of g_m between ZrO_2 and the test structures

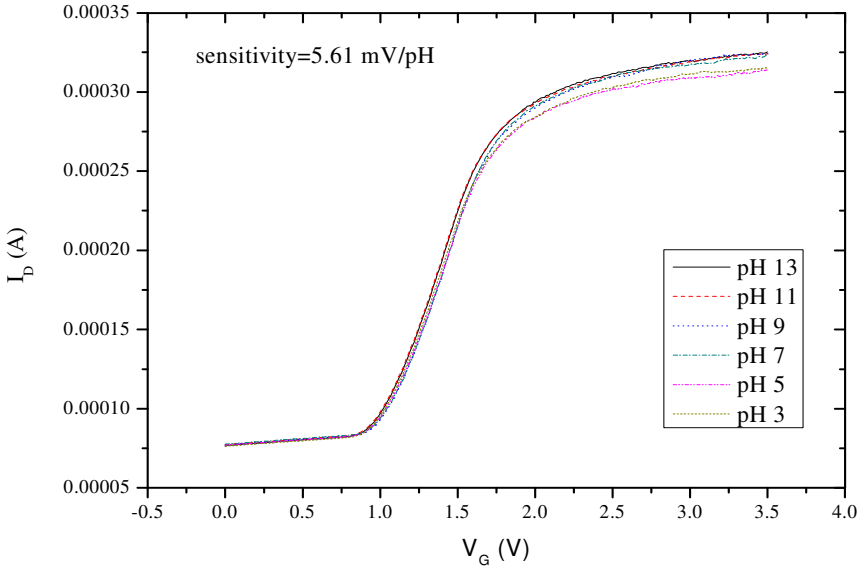

Fig. 4-20 Selectivity of the PR/HMDS/ZrO_2 structure

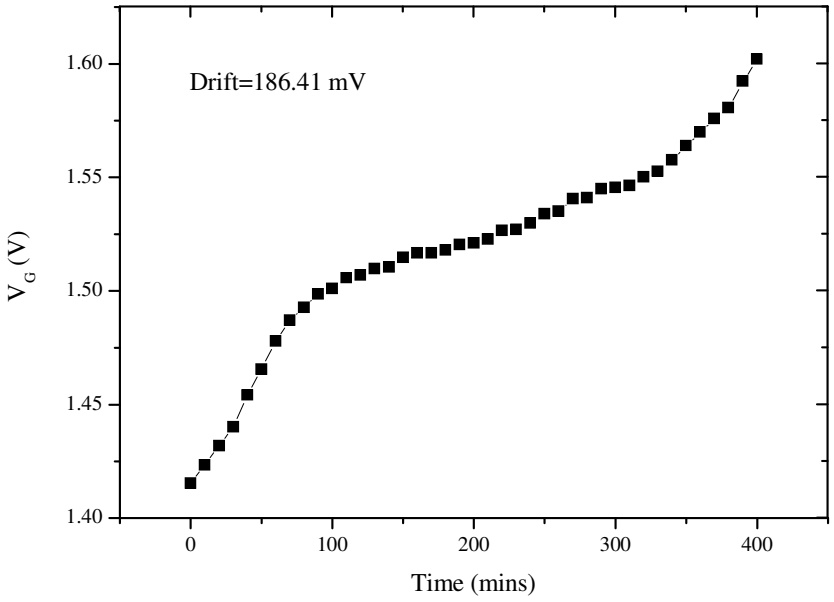

Fig. 4-21 Time to drift in pH 7 buffer solution of the PR/HMDS/ZrO_2 structure for 400 minutes

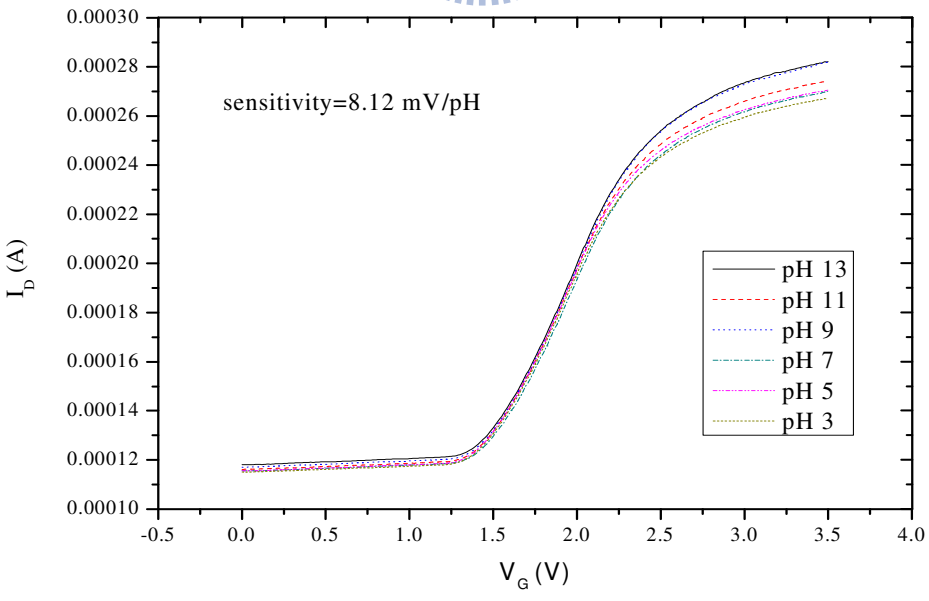

Fig. 4-22 Sensitivity of the mixture (Nafion1:polyimide1)/HMDS/ZrO_2 structure

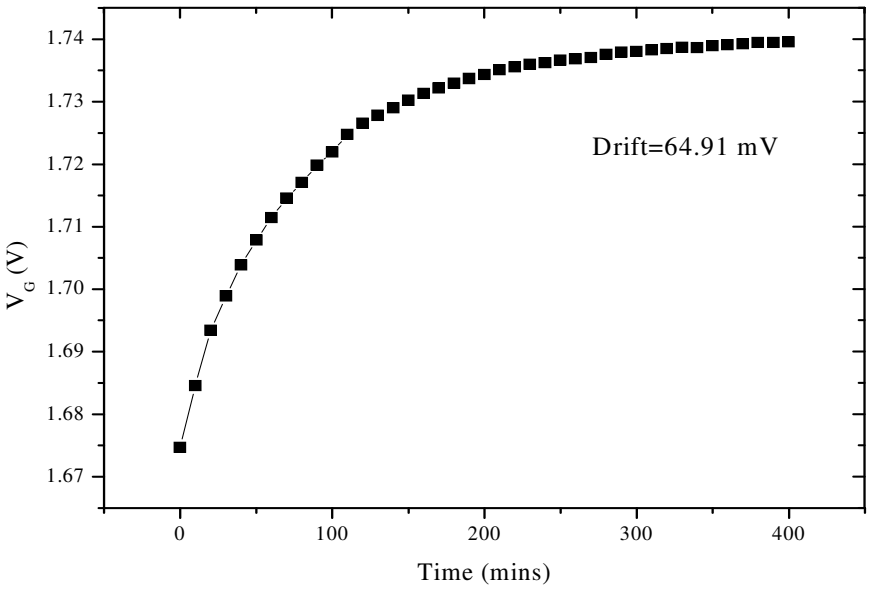

Fig. 4-23 Time to drift in pH 7 buffer solution of the mixture (Nafion1:polyimide1)/HMDS/ZrO_2 structure for 400 minutes

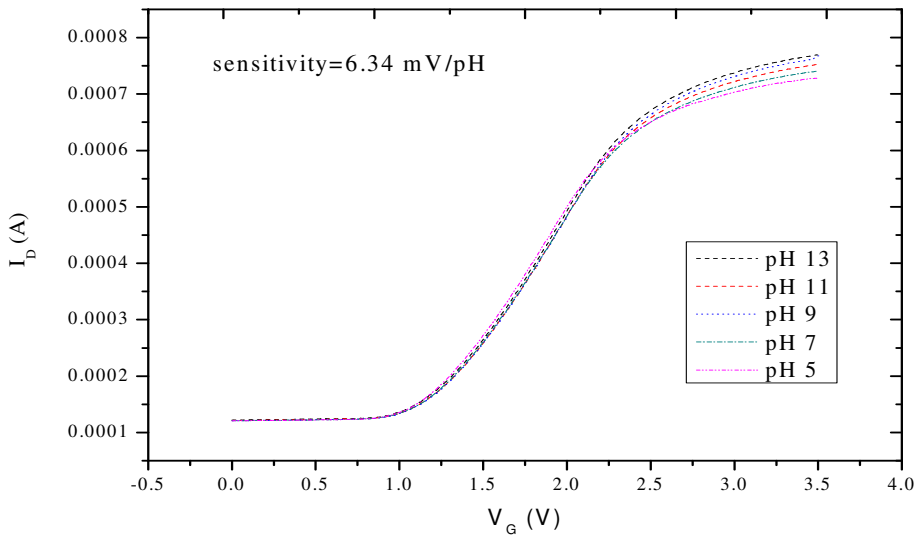

Fig. 4-24 Sensitivity of the mixture (Nafion1:polyimide3)/HMDS/ZrO_2 structure

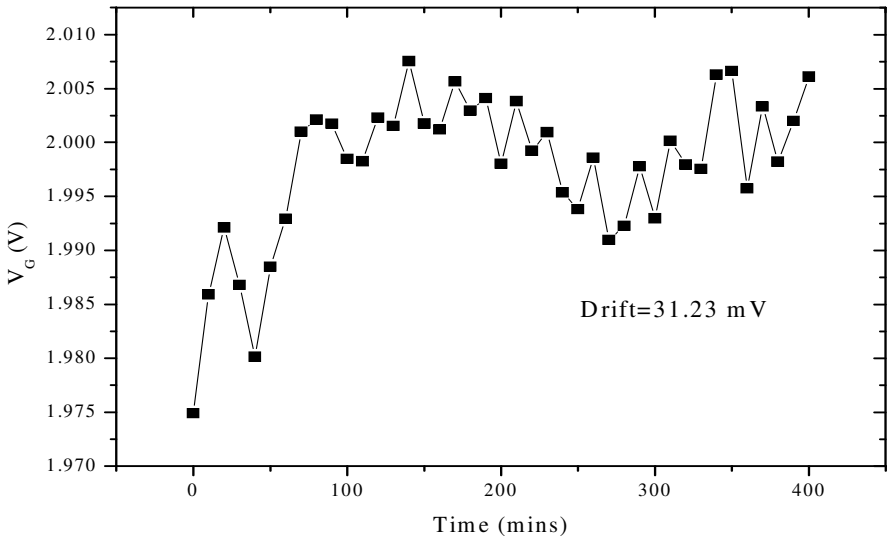

Fig. 4-25 Time to drift in pH 7 buffer solution of the mixture (Nafion1:polyimide3)/HMDS/ZrO_2 structure for 400 minutes

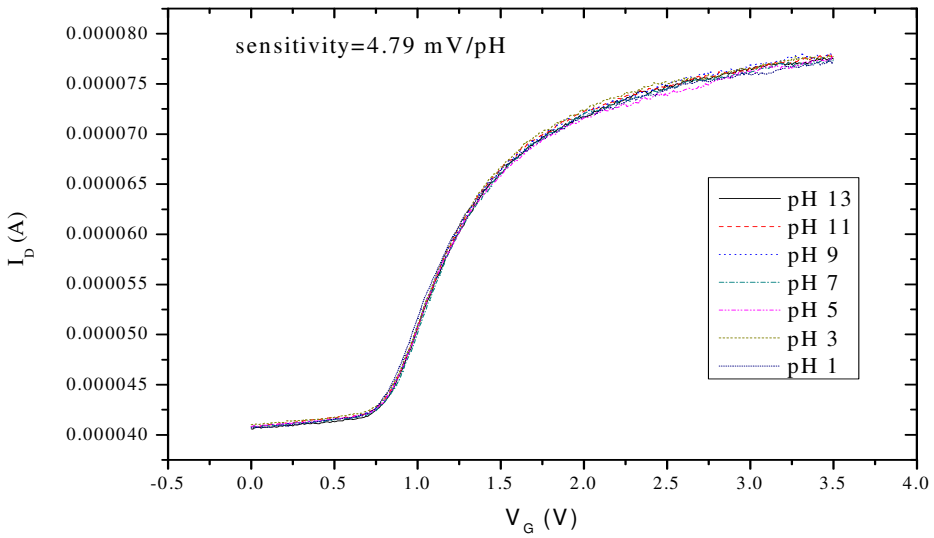

Fig. 4-26 Sensitivity of the polyimide/HMDS/ZrO_2 structure

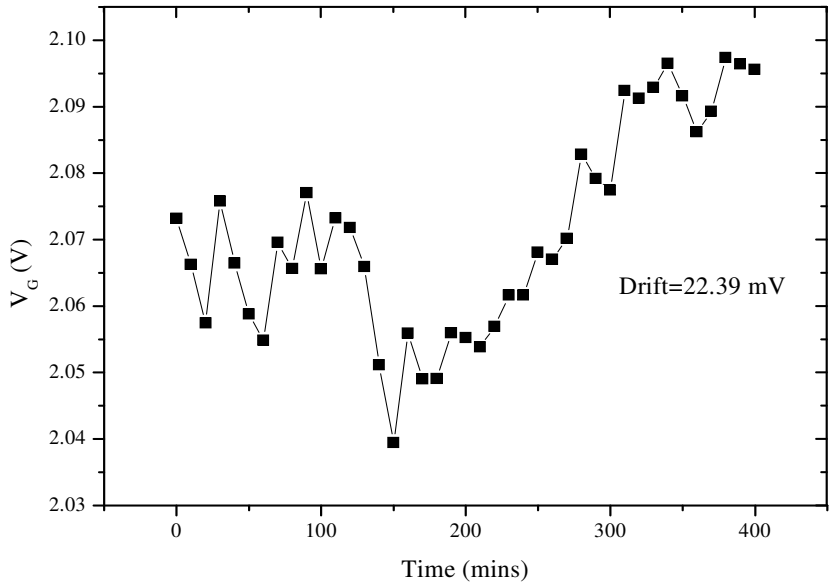

Fig. 4-27 Time to drift in pH 7 buffer solution of the polyimide/HMDS/ZrO_2 structure for 400 minutes

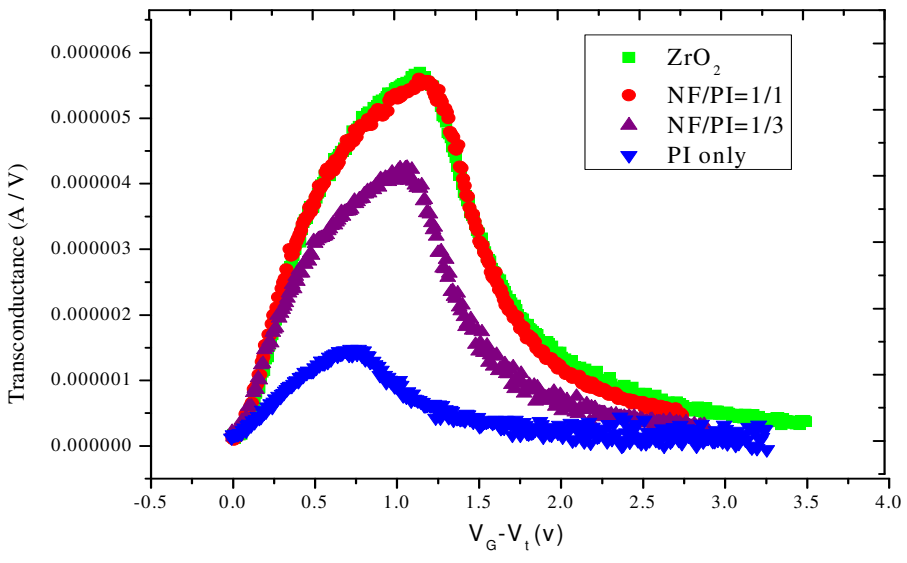

Fig. 4-28 Comparison of g_m between ZrO_2 and the test structures

Table 1-1 Sensitivities and test range for different sensing membranes

Sensing membrane	Test range(pH)	Sensitivity(mV/pH)	Reference
ZrO_2	1-13	57.5	4
Si_3N_4	1-13	46-56	5
Al_2O_3	1-13	53-57	6
Ta_2O_5	1-13	56-57	7
SnO_2	2-10	58	8

Table 3-1 Specifications of wafers

Diameter (mm): 100+/-0.5	Diameter (mm): 100+/-0.5
Type/Dopant : P/Boron	Type/Dopant : P/Phosphorous
Orientation : <100>	Orientation : <100>
Resistivity (ohm-cm):1-10	Resistivity (ohm-cm):1-12
Thickness (μ m) ：505-545	Thickness (μ m) ：515545
Grade : Prime	Grade : Prime

Table 3-2 Parameters of sensing layers deposition with sputter

parameters of ZrO_2 sputter
power : 110 W
Ar/O_2 : 24/8 (sccm)
Density : 6.51
Acoustic impendance : 14.72
Tooling factor : 0.533
Rate : 0.01 Å/s
pre sputter 60W for 10 min
Pressure : 7.6×10^{-3}

Table 3-3 The test structures of REFET, NF=Nafion, and PI=polyimide

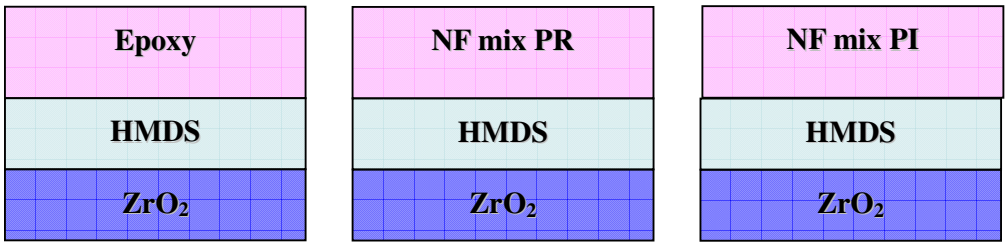

Table 4-1 Sensitivity at the optimum operation current

	p-type pH-ISFET	n-type pH-ISFET
Sensitivity/ operation current	57.08 mV/pH/ -147.45 μA	58.73mV/pH/ 71.7 μA

Table 4-2 Comparison between original and modified *S / N* ratio

	S/N| p-type ISFET	S/N| n-type ISFET	Modified S/N
pH 5	440.45	560.25	6259.92
pH 7	293.73	280.11	2094.5
pH 9	433.95	327.82	1422.21
pH 11	272.55	180.65	635.05
Average	360.17	337.21	2602.93

Table 4-3 Parameters of the test structures; NF=Nafion, PI=polyimide

	Epoxy/HMDS/ZrO_2	PR mixed NF/HMDS/ZrO_2	PI mixed NF/HMDS/ZrO_2
Sensitivity (mV/pH)	14.03	5.61	8.12
Drift rate (mV/hr)	N.A.	27.96	9.74

Table 4-4 Parameters of the test structures; NF=Nafion, PI=polyimide

	mixture(NF1:PI1) /HMDS/ZrO_2	mixture(NF1:PI3) /HMDS/ZrO_2	PI /HMDS/ZrO_2
Sensitivity (mV/pH)	8.12	6.34	4.79
Drift rate (mV/hr)	9.74	4.68	3.36